Spring 5-3-2024

Engineering a Compostable Isolation Gown to Reduce Hospital-Derived Synthetic Waste Accumulation in Landfill

Caden A. Scott
University of Maine, caden.scott@maine.edu

ENGINEERING A COMPOSTABLE ISOLATION GOWN TO REDUCE HOSPITAL-DERIVED SYNTHETIC WASTE ACCUMULATION IN LANDFILL

By

Caden Scott

B.S. University of Maine, 2022

A THESIS

Submitted in Partial Fulfillment of the

Requirements for the Degree of

Master of Science

(in Biomedical Engineering)

The Graduate School

The University of Maine

May 2024

Advisory Committee:

David J. Neivandt, Professor of Chemical and Biomedical Engineering, Advisor

Deborah A. Saber, Associate Professor of Nursing

Jean D. MacRae, Associate Professor of Civil and Environmental Engineering

ENGINEERING A COMPOSTABLE ISOLATION GOWN TO REDUCE HOSPITAL-DERIVED SYNTHETIC WASTE ACCUMULATION IN LANDFILL

By Caden Scott

Thesis Advisor: Dr. David J. Neivandt

An Abstract of the Thesis Presented
in Partial Fulfillment of the Requirements for the
Degree of Master of Science
(in Biomedical Engineering)
May 2024

The ever-increasing accumulation of synthetic waste in landfills is a growing pollution and public health concern. In 2018, hospitals in the United States landfilled 1.5 million tons of personal protective equipment (PPE). Single-use, disposable PPE gowns constitute the greatest percentage of landfilled PPE by weight and are overwhelmingly made from non-degradable synthetic polymer materials. The most common and disposed of type of PPE gown is isolation gowns, which are used by healthcare workers attending patients under isolation precautions. One study has shown that under isolation procedures, healthcare systems will on average dispose of 33 gowns per patient per day as municipal waste, contributing a substantial amount of solid waste to landfills. Therefore, to alleviate the strain on landfills, a need exists for isolation gowns that do not contribute to the accumulation of synthetic waste. The approach taken in the present work to address this need was through the creation of a degradable textile from which to fabricate isolation gowns. The UM39 textile is a paper-based substrate with a compostable functional coating to grant the barrier properties necessary to prevent liquid penetration. The compostable, lightweight, coated paper product was tested in accordance with the ASTM F3352 Standard Specification for Isolation Gowns Intended for Use in Healthcare Facilities. The UM39 material was found to exceed the

physical strength requirements and possess better barrier properties than most commonly used isolation gowns. In addition, the UM39 material was demonstrated to exhibit qualitative and quantitative signs of degradation after 42 days under industrial composting conditions. Due to these properties, the UM39 textile has been identified as a suitable material from which to create compostable isolation gowns. To confirm the material's potential to replace traditional synthetic polymer-based gowns, a full-sized, PB70 Level 3 compliant prototype UM39 isolation gown was fabricated.

Dedicated to Apollo

Wherever you are, I hope you like the music

ACKNOWLEDGEMENTS

Firstly, I would like to thank Dr. David Neivandt for his incredible mentorship. As an advisor, he continually pushed me to my best and gave me the opportunity to grow as both a researcher and a leader (and he's not half bad at digging holes in windrows). I attribute much of my growth over the last two years to his mentorship.

I would also like to express my appreciation for my thesis committee members Dr. Deborah Saber and Dr. Jean MacRae for their expertise and assistance. Without Dr. Saber's clinical perspective and knowledge, this project would not have been possible.

Furthermore, I am incredibly grateful for the support of our amazing collaborators Mantrose-Haeuser, St. Croix Tissue, Maine-Lee Technology Group, and Casella Organics Hawk Ridge. I also would like to thank the Paper Surface Science Program and Process Development Center at the University of Maine for access to their equipment and training as well as the Maine Technology Institute for funding.

On a personal note, I would like to acknowledge my best friend Grace Johnson for being the shining light in the dark sea of thesis writing, reminding me what I am doing this for. Lastly, and most importantly, I would like to thank my parents, Alana and Michael Jette, for always being in my corner. Your selflessness inspires me every day.

TABLE OF CONTENTS

TABLE OF FIGURES

TABLE OF TABLES

CHAPTER ONE: Introduction

1.1 Hospital-derived Synthetic Waste

The ever-increasing accumulation of non-degradable waste in landfills is a growing pollution and public health concern.[1] In 2018, 292.4 million tons of municipal solid waste (MSW) were generated in the United States, with 146 million tons being directly landfilled.[2] Landfills are designated solid waste accumulation sites and have been identified as a threat to the surrounding environment due to their contaminants leaching into the groundwater and polluting the air.[3–6] While landfill engineering has advanced in recent years to mitigate the environmental effects of these facilities to some extent, landfills have retained the potential to cause harm in neighboring populations.[7–9] For example, a link between the airborne landfill contaminant H_2S and respiratory diseases has been demonstrated, which has been found to particularly affect those living in proximity to landfills.[10] As the accumulation of solid waste increases, landfills will grow in both size and number, potentially emitting a greater number of contaminants to a larger population.

A significant portion of the solid waste accumulation in landfills is attributable to the increase in synthetic materials used in manufacturing. In 2018, 17 million tons of textile waste were created, comprising 5.8% of the total MSW generation in the United States that year.[11] Of these 17 million tons, 11.3 million tons were directly landfilled, representing an almost tenfold increase since 1960.[11] Furthermore, due to the prevalence of synthetic materials in textiles, such as polyester and polypropylene, many textiles may not degrade for decades.[12,13] As such, it is projected that synthetics in textiles will continue to accumulate as more waste is added to landfills each year.[14]

A major source of textile waste in landfills is from health care systems. Hospitals in the United States are estimated to produce 6 million tons of waste annually, with 25% being directly landfilled plastics including personal protective equipment (PPE).[15,16] PPE consists of specialized items of clothing worn by healthcare workers to minimize the risk of the transfer of solid, liquid, or air-borne contagions.[17] PPE is commonly designed to be immediately disposed of upon end of use and therefore contributes heavily to a hospital's waste.[18,19] Furthermore, PPE is generally made of non-compostable plastics due to synthetic polymers' cost-effectiveness, barrier properties, and ability to be sterilized.[20] The combination of these properties has made synthetic polymers a ubiquitous material for PPE, regardless of their environmental impacts.

1.2 Isolation Gowns

1.2.1 Role of Isolation Gowns

The majority of hospital PPE waste by weight is gowns.[21] Gowns are used by healthcare workers to cover the torso, arms, and legs from potentially infectious fluids and particles that may be encountered while treating patients.[22] Gowns typically fall into two categories: surgical and isolation, with isolation comprising up to 85% of PPE waste by weight.[21] Surgical gowns and isolation gowns serve a similar purpose in protecting healthcare workers and patients, however, the former are designed for use during surgical operations and are typically heavier and grant greater protection than isolation gowns.[17] As such, surgical gowns are primarily reserved for sterile, high-fluid level situations with risk of blood exposure, whereas isolation gowns are used for more commonplace non-sterile patient care in acute, rehabilitation, and long-term healthcare facilities.[17,23]

Isolation gowns are used as a result of strict protocols enacted for patients with especially dangerous or contagious infections such as antibiotic resistant Methicillin-resistant

Staphylococcus aureus (MRSA).[24] When subject to isolation procedures, patients are either placed in a sole occupancy room, or with other isolated patients, with any attending healthcare worker or visitor donning an isolation gown upon entering and doffing before leaving.[25–27] In addition to strictly hospital settings, isolation gowns are used for various PPE applications in healthcare more broadly. The United States Centers for Disease Control, for example, has recently recommended the use of isolation gowns in nursing homes to reduce the rising prevalence of multidrug-resistant organism colonization among nursing home residents.[23] Furthermore, isolation gowns are routinely used in oncology and dialysis clinics to reduce the chance of spreading infections to immunocompromised patients.[28,29] The majority of such gowns are single-use disposable.[30,31] While there has been a push in recent years for reusable gowns, the barrier properties of reusable gowns on the market have been found to diminish to unacceptable levels with successive washings.[31–34] Furthermore, regardless of reusability, once isolation gowns are disposed of, unless they are soaked with blood, they are sorted into MSW.[35] Gowns that become soaked with blood, which is more common for surgical gowns than isolation gowns, are disposed of as biohazardous waste and incinerated.[35] Isolation gowns sorted into MSW are subsequently landfilled and are a major contributor to the accumulation of synthetic non-compostable waste.[36]

1.2.2 Requirements of Isolation Gowns

To be used in hospitals, isolation gowns must meet the standard put forth by ASTM International, the organization formerly known as the American Society for Testing and Materials. ASTM International creates uniform testing procedures and reporting requirements such that end users are able to make an informed purchase of items that adhere to specific standardized properties. For isolation gowns, these properties can be divided into two categories:

barrier and physical. Barrier properties describe the extent of liquid penetration through the gown, while physical properties describe the strength of the material.

The ASTM standard for isolation gowns, F3352, uses a number of tests to determine the degree of barrier protection afforded by an isolation gown. Barrier tests are used to find the Association for the Advancement of Medical Instrumentation (AAMI) Protective Barriers 70 (PB70) Level. The PB70 Level is a numeric indicator from 1 to 4 that describes the minimum barrier performance of gowns and other protective apparel, with Level 1 granting the least protection and Level 4 granting the most protection. The three tests used to determine a material's PB70 Level include the American Association of Textile Chemists and Colorists (AATCC) 42 Impact Penetration Test, the AATCC 127 Hydrostatic Pressure Test, and the ASTM F1671 Bacteriophage Penetration Test. The results of these three tests are compared to the minimum or maximum values required for each Level. The requirements of the ASTM F3352 standard for each PB70 Level are summarized in **Figure 1.1**.

Barrier Performance and Physical Property Performance Requirements of Single and Multiple-Use Isolation Gowns

Property	Test Method	AAMI PB70 Level			
		1	2	3	4
Barrier Performance	AATCC 42	≤ 4.5 g	≤ 1.0 g	≤ 1.0 g	N/A
	AATCC 127	N/A	≥ 20 cm	≥ 50 cm	N/A
	ASTM F1671	N/A	N/A	N/A	Pass
Tensile Strength	ASTM D5034	≥ 30 N	≥ 30 N	≥ 30 N	≥ 30 N
Tear Strength	ASTM D5733	≥ 10 N	≥ 10 N	≥ 10 N	≥ 10 N
Seam Strength	ASTM D1683	≥ 30 N	≥ 30 N	≥ 30 N	≥ 30 N

Figure 1.1. Barrier and Physical Property Requirements detailed in the ASTM F3352 Standard Specification for Isolation Gowns Intended for Use in Healthcare Facilities. Modified from Ref [37].

For a particular Level of protection, all three barrier tests must meet the minimum or maximum values required for that specified Level. Furthermore, as isolation gowns must provide full coverage, the seams of the gown must also be tested and meet the same requirements as the continuous fabric of the gown.[37]

1.3 Need for a High-Protection Degradable Gown

1.3.1 Number of Gowns

While isolation gowns are a crucial component of hospital safety protocols in place to protect healthcare workers and patients, the vast amount of synthetic waste generated by their use produces significant quantities of non-degradable material. One study conducting a waste audit in an intensive care unit (ICU) determined that an average of 33 gowns per patient per day are utilized for a stable patient under isolation precautions; the number of gowns used is likely much higher for unstable patients, as unstable patients require more frequent care and examination.[21] As such, extrapolating the figure in this waste audit to the number of ICU beds in the United States may provide an estimate for the number of isolation gowns used in ICUs each year. The Healthcare Provider Cost Reporting Information System (HCRIS) reports that in 2017 there were 103,900 ICU beds in hospitals in the United States.[38] From the Society of Critical Care Medicine's (SCCM) analysis of the number of the reported days the ICU beds were used, an ICU bed occupancy rate of 66% was approximated.[39] The combination of statistics from the waste audit, HCRIS report, and SCCM analysis is able to provide an estimate of 25,029,510 isolation gowns used in ICUs each year in the United States. The number of gowns used each year is likely much higher due to the use of isolation gowns in less acute areas of care such as dialysis clinics and nursing homes. As such, an alternative method of determining the number of gowns used in healthcare settings may provide a more realistic estimate.

Another method to approximate the number of gowns contributed to landfills may be the cumulative total of gowns purchased. By extrapolating the number of gowns purchased per bed in Maine hospitals to the nationwide number of hospital beds, an estimated 2.5 billion gowns were purchased in the United States in 2022.[40] As gowns continue to be purchased each year, the overwhelming majority of the purchased gowns can be assumed to be used, and thereby contribute to synthetic waste accumulation in landfills. The difference between the two estimates is likely reasonable due to the second estimation incorporating the use of isolation gowns outside ICU settings and the greater need for isolation gowns for more acute patients. As such, it is reasonable to assume that over 2 billion gowns per year are landfilled, leading to an immense need for an eco-friendlier alternative.

1.3.2 PB70 Level of Gowns

The need for a re-engineered isolation gown is strengthened by the fact that previous studies have demonstrated that a number of the gowns currently on the market do not meet the required ASTM performance specifications.[33,41,42] As stated in Section 1.2.2, the degree of barrier protection a gown provides is classified using the AAMI PB70 Level.[43] Current isolation gowns typically fall under Level 1 or Level 2 and a number have been demonstrated to not provide adequate protection to the user.[44] The underperformance of the tested Level 1 and Level 2 gowns has contributed to the recent recommendations by one research group to use Level 3 gowns for isolation protocols as they possess a higher degree of barrier protection.[45]

Therefore, to provide an alternative to current underperforming isolation gowns that result in the accumulation of nearly one hundred thousand tons of non-degradable plastic waste in landfills, a compelling need exists for a degradable isolation gown with Level 3 barrier protection.

1.4 Potential Disposal Pathways of Personal Protective Equipment

1.4.1 Modern Landfills

To design a degradable isolation gown, the target degradation pathway must be identified. Traditional synthetic polymer-based isolation gowns that are not soaked with blood are discarded as municipal solid waste (MSW) and eventually landfilled.[35] Modern MSW landfills are designated accumulation sites of waste which are lined with clay and plastic to prevent contaminated rainwater from leaching out from the landfill.[46] However, the purpose of an MSW landfill is commonly not just to provide an area of land on which to store MSW, but also to act as a source of energy generation through the methane gas produced by the waste via anaerobic degradation. Once a landfill has reached its storage capacity, it is covered with layers of soil and clay to contain the waste.[46] **Figure 1.2** presents a diagram of a cross-sectional view of a finished, closed landfill.

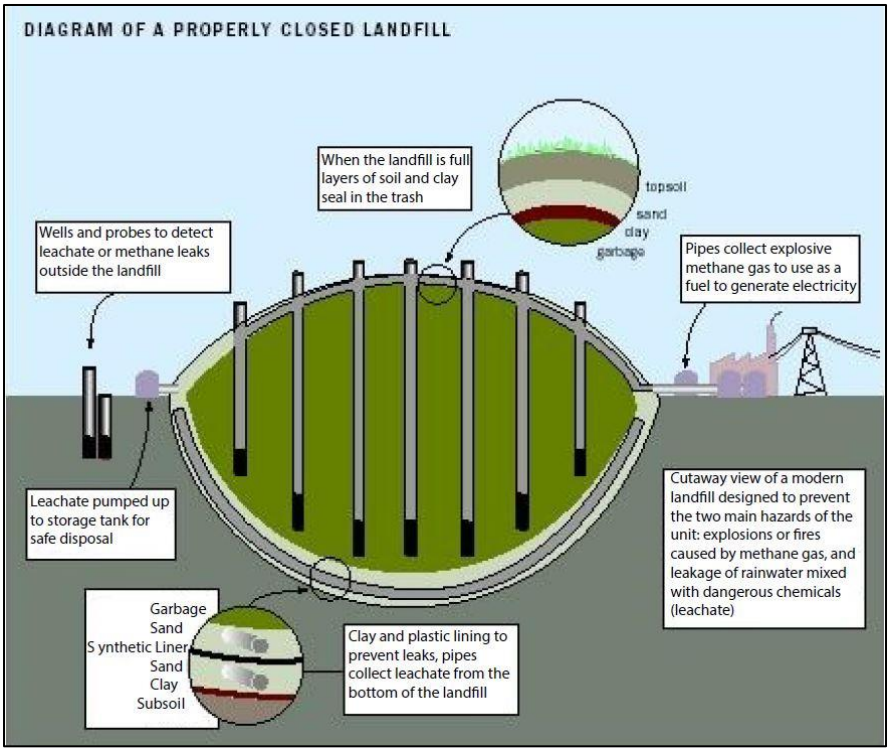

Figure 1.2. Cross-sectional view of a closed MSW landfill where pipes are used to collect methane gas from the enclosed waste. Reproduced from Ref [46].

Once the landfill is covered, pipes are inserted into the closed landfill to collect methane gas, which can be used as fuel to generate electricity. However, although modern engineering has allowed for the creation of landfills that produce a useful byproduct, a number of disadvantages persist that make landfill accumulation of synthetic waste an imperfect solution. Firstly, despite measures such as wells and probes in use to detect leaks from a closed landfill, hazardous liquid resulting from rainwater percolating through a solid waste disposal site will inevitably be generated. [47] Leachate from MSW landfills has been shown to negatively impact surrounding groundwater and no method currently exists to completely eliminate leachate emission from landfills.[3–6,48,49] In addition to the issue of leachate, in order to generate methane gas, traditional sealed landfills exclude oxygen and water to create anaerobic conditions.[50] Therefore, biological degradation is severely limited inside the landfill, leading to landfills

operating as waste holding facilities rather than waste degradation facilities. As such, the landfilled waste is designed to remain in the landfill, rather than degrade over time, thereby permanently precluding the landfill site from any other usage.

To provide an eco-friendlier alternative to traditional MSW landfills, the United States Environmental Protection Agency has recently conducted pilot-scale trials of bioreactor landfills.[51] Bioreactor landfills inject a mixture of recirculated leachate, stormwater, and wastewater back into the landfill to promote microbial activity, increase the rate of degradation of landfilled materials, and reduce leachate discharge into the environment.[51] However, bioreactor landfills continue to discharge leachate and cannot degrade synthetic polymer materials as quickly as they are industrially produced.[52] As such, despite advancements in technology, MSW landfills continue to produce harmful effects on their surrounding environment. Furthermore, issues arise in the amount and type of land required to build a landfill. In addition to the approximately 750 acres of land required to construct a landfill site, landfills cannot be built near geologic faults, wetlands, flood plains, or residential areas.[46,53] The combination of these land restrictions results in great difficulty for MSW landfills to be constructed near metropolitan areas, which generate the most MSW, leading to high transportation costs and logistical difficulties in waste disposal.[54] Furthermore, as synthetic polymer materials take decades to degrade, the current rate of plastic production severely outpaces its degradation.[52] Therefore, the sole utilization of landfills to address the current rate of production of synthetic waste is not a viable long-term solution as eventually there would no longer be suitable land from which to construct a landfill. As such, landfill disposal was excluded as the target degradation pathway in the design of a degradable isolation gown.

1.4.2 Incineration and Pyrolysis

After landfilling, the next most common disposal pathway for medical gowns is incineration.[35] Incineration consists of the combustion of material under high temperatures (approximately 1000°C) in the presence of oxygen and is used to sterilize biohazardous waste and significantly reduce its mass.[55] Many hospitals contain on-site incinerators which burn biohazardous waste into ash.[56,57] Unfortunately, the burning of the synthetic materials commonly used in PPE manufacturing produces poisonous gases and toxic metal ash, such as carbon monoxide and polychlorinated dibenzo-dioxins, respectively.[58] Furthermore, the resulting ashes are subsequently landfilled, leading to the same negative outcomes previously summarized in Section 1.4.1.

To mitigate the problems inherent to incineration, recent studies have been conducted regarding the applicability of pyrolysis. Pyrolysis, unlike incineration, is an anaerobic process which targets the breaking of chemical bonds in polymeric materials to convert waste into usable products.[59,60] Pyrolysis is performed in a temperature range of 400-600°C, via application of heat to synthetic polymer waste in oxygen-deprived environments. The process has been shown to convert the organic components in the waste to oils similar in properties to crude oil derived from fossil fuels.[59,61] Although a promising method to reduce the accumulation of synthetic waste, a number of challenges persist in transitioning pyrolysis reactors to the industrial scale. The heterogeneity of feedstock from different synthetic polymer waste streams can cause significant issues; for example, the simultaneous pyrolysis of PET and PVC, two common synthetic polymer materials, produces organic chlorine compounds which reduce the quality of the resultant oil.[62] Furthermore, due to the heterogeneity of the feedstock, oil derived from pyrolysis can vary significantly in composition and quality compared to fossil fuel derived oils.[62]

As such, while pyrolysis has been demonstrated to potentially be a promising method of converting PPE gowns made from synthetic polymeric materials into a usable product, numerous challenges remain to realize pyrolysis on an industrial scale. Therefore, pyrolysis was also excluded as a potential degradation pathway in the design of a degradable isolation gown.

1.4.3 Biodegradation and Composting

Composting entails the microbial degradation of organic materials under aerobic conditions to produce CO_2, H_2O, compost, and humus.[63,64] While the term compost can be applied to materials undergoing the composting process, humus refers to the nutrient-rich, stable, organic product resulting from the process.[65] A generalized diagram of the composting process is presented in **Figure 1.3**.

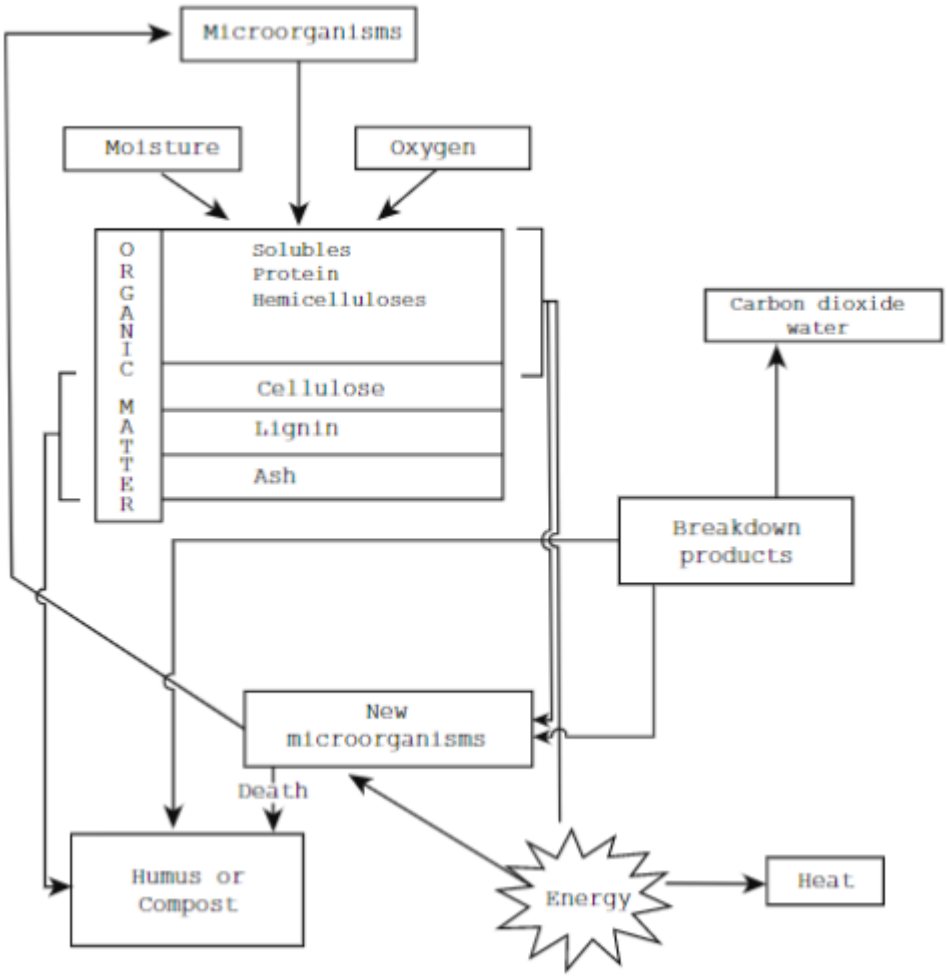

Figure 1.3. Generalized diagram of the composting process. Reproduced from Ref [70].

Figure 1.3 details a simplified abstraction of the complex composting process. Organic matter is exposed to moisture, oxygen, and microorganisms. The types of microorganisms include bacteria, actinomycetales (a gram positive filamentous order of bacteria commonly found in aerobic environments), and fungi.[64,66–68] Although bacteria are the dominant type of microorganism found in compost (~80-90%), fungal microorganisms also assist in the microbial breakdown of material.[63,69] An extensive list of the bacterial, actinomycetal, and fungal microorganisms typically found in compost is presented in **Appendix A.1**.[64] Once exposed, the organic matter is subsequently broken down and digested by the microbes, producing energy for microbial proliferation and exuding heat.[70] The rate of degradation is variable according to the

specific microbes in the compost, environmental factors such as temperature, humidity, oxygen concentration, pH, and UV radiation, as well as the properties of the composted material.[71] The optimal values of the environmental factors to facilitate microbial degradation of compost depend on the specific microbes as well as the stage of the decomposition of the compost.[72] However, the prominent process limitations of microbial degradation in industrial composting include low moisture, low oxygen concentration, and a lack of available carbon or degradable organics.[64] The general byproducts of composting include CO_2, H_2O, humus, and compost; the products, however, can vary depending on the specific microbes and feedstock.[72] The humus, a nutrient-rich organic fertilizer, is subsequently able to be applied to agricultural soil to promote plant growth.

In addition to generating a useful agricultural product, benefits of composting also include the sequestration of carbon into soil and the suppression of plant diseases caused by soil-borne pathogens through antibiosis and other mechanisms.[64,73] Although greenhouse gases such as CO_2, NH_3, and methane are released during the composting process, it is generally accepted that composting results in less greenhouse gas emissions than landfilling.[74] However, as the complex microbial mechanisms are not fully understood and can vary with feedstock, a quantitative comparison cannot be made.[74] Compared to the previously discussed degradation methods that depend on the fabrication of synthetic polymeric materials for feedstock to produce useful products, composting pathways offer an eco-friendlier alternative. Biodegradable and compostable materials are defined by their ability to be degraded through the action of biological agents such as fungi and bacteria.[71] While all compostable materials are biodegradable, not all biodegradable materials are compostable. To be classified as compostable, a material must be biodegradable and meet a series of ASTM and ISO standards that dictate a number of tests to

quantify a material's rate of degradation, toxicity, and byproducts under controlled laboratory composting conditions. As such, the main drawback of using composting processes for waste management is illuminated: not all materials are able to be industrially composted.

Regardless of the inherent limitations of compost degradation, many industrial composting facilities exist to convert organic biomass into useable compost/humus. One such facility is Casella Organics Hawk Ridge in Unity, Maine. Hawk Ridge is an industrial composting facility that converts biowaste into compost through an in-vessel GICOM Dutch Tunnel system and windrow curing.[75] The Dutch Tunnel aerates a mixture of municipal sewage sludge, wood shavings, sawdust, and an inoculant of previously finished compost for a period of 7-14 days, referred to as the active composting phase. The mixture is subsequently formed into windrows, which are 160ft long, 14ft wide, and 10ft high rows of composted material. In the windrow phase, microbes in the environment break down the organic material remaining in the windrow for a period of approximately 40 days. The resulting compost/humus is subsequently sold to agricultural or industrial companies as a fertilizer for plant growth.

Industrial composting facilities possess a number of advantages over modern landfill or pyrolysis techniques for waste management. Firstly, in direct contrast to landfills, composting is designed to accelerate biological degradation. As such, compost does not accumulate in industrial facilities as waste accumulates in landfills, as the compost is continually sold as a product. Furthermore, relative to pyrolysis, industrial composting facilities have a much greater tolerance of the heterogeneity of their feedstock.[64] As such, composting facilities are able to process feedstocks from diverse waste streams. Due to the many advantages of industrial composting over pyrolysis or landfill waste disposal pathways, composting was identified as the

target degradation pathway of the degradable PPE gown. Therefore, the exclusive use of organic, compostable materials was implemented as a design constraint.

1.5 Current Degradable Gowns and Reusable Gowns

1.5.1 Reusable Gowns

Current methods to reduce the amount of synthetic PPE waste from healthcare systems include the use of reusable and degradable gowns. Reusable gowns constitute approximately 20% of gowns on the market.[33] The domination of single-use disposable gowns over reusable gowns on the market is due to a number of factors such as the increased cost, laundering needs, and the reduction of barrier properties over time inherent to reusable gowns.[33,76,77] As of 2024, Level 1 and 2 single-use polypropylene and polyethylene gowns can be purchased for approximately $1.20 per gown, with Level 3 gowns costing approximately $3.75 per gown.[78–81] Reusable gowns, however, cost more per unit; two representative commercially available Level 2 and Level 3 gowns are available to be purchased for $8.52 and $10 per gown, respectively.[77,82] The sevenfold increase in price for Level 2 single-use vs reusable gowns makes transitioning from single-use to reusable gowns a difficult to justify investment for healthcare purchasers. Although less reusable gowns would be required to be purchased compared to single-use disposable gowns, the need for laundering reusable gowns adds cost to their integration. Specifically, cleaning the gowns for reuse in on-site laundering facilities requires labor, machine maintenance, and water and power consumption, which can be prohibitive to healthcare systems converting to reusable gowns.[76] Furthermore, the barrier properties of reusable medical textiles have been shown in multiple studies to decrease after 50 industrial washings.[31–34] As such, although the full integration of reusable gowns may significantly decrease the number of PPE gowns landfilled each year, a number of challenges persist in their implementation.

1.5.2 Degradable Gowns

As an alternative approach to reduce the synthetic polymer-derived waste produced by healthcare systems, a number of companies have developed sustainability-driven single-use disposable PPE. The GoGreen gown, developed by PPE Plus, is marketed as a Level 3 biodegradable isolation gown which fully decomposes after 6 months in a landfill.[83] However, the product's material is described as a biodegradable polyethylene, which is a synthetic polymer. Previous research has demonstrated that although biodegradable synthetic polymers that can be broken down by microbial action have been developed, the resulting degradation produces microplastics that have been found to produce adverse environmental effects.[52,71] Another biodegradable isolation gown, the KF-IG AP2G, sold by Kingfa Science and Technology Company, claims 94% degradation after 90 days presumably under landfill conditions.[84] However, the component materials of the KF-IG AP2G are listed as PBAT and PLA. While both materials are considered to be biodegradable plastics, synthetic polluting materials are used in their fabrication, and thus provide an imperfect solution towards creating a fully sustainable product.[85] The Biogown, produced by TerraLoam, is manufactured from corn starch and biodegradable polymers.[86] TerraLoam's process describes an option for healthcare systems upon disposal of the gown to either return the used Biogowns to TerraLoam for composting over a period of 3-4 months or discard the gowns to an open-air landfill to degrade over a period of 12-18 months.[86] While biodegradable, the Biogown is not certified to be industrially compostable. Consequently, the Biogown is unable to be accepted as feedstock for general industrial composting processes, therefore continuing to necessitate the use of landfills.

1.6 Approach

In all, a pressing need exists to address the environmental and public health challenges posed by the accumulation of non-degradable synthetic polymer PPE gown waste in landfills. Current methods to address this need, namely reusable and biodegradable gowns, continue to exhibit a number of challenges such as cost, microplastic generation, not meeting ASTM compostability standards, and insufficient barrier properties. As such, a significant gap in the market exists for a high-protection, degradable, disposable isolation gown manufactured from solely non-synthetic materials. Through the evaluation of potential disposal methods, composting was determined to be the most sustainable and practical degradation pathway for used isolation gowns. Therefore, the approach taken to address the gap in the market was the development of a PB70 Level 3 compliant PPE gown fabricated from industrially compostable materials. Specifically, a coated paper gown of an inherently biodegradable cellulosic paper base and functional coating certified to be industrially compostable was designed and fabricated.

CHAPTER TWO: Materials and Methods

2.1 Materials

A series of substrates of varying basis weights and compositions, in addition to coating formulations, were evaluated and compared to an on-market polypropylene HARBL3 Class 3 isolation gown.[87] Commercial tissue and hand towel formulations were targeted as potential substrates due to their inherent biodegradability as well as their soft, pliable, and lightweight yet strong qualities. As such, these substrates were likely to grant the required physical strength properties while maximizing wearability. From extensive testing of a variety of paper substrates of basis weights ranging from 18 grams per square meter (gsm) to 44gsm provided by St. Croix Tissue in Baileyville, Maine, two substrates, 29gsm and 39gsm, were selected for further investigation based on their degree of coating absorption as well as their texture and flexibility once coated. Basis weight samples less than 29gsm were found to shrink when saturated with coating, and basis weight samples greater than 39gsm demonstrated a high degree of stiffness and roughness after coating. In addition, the coating used for the final prototype underwent multiple reformulations to increase pliability of the coated product while retaining its barrier properties. Through the assessment of different combinations of substrates and coatings according to the F3352 standard, the UM39 prototype was found to grant the greatest barrier properties relative to its weight. The results of material testing of another such prototype, the lighter UM29, are also shown for comparative purposes.

The UM39 prototype textile was fabricated from two components: a paper substrate and a functional coating. The paper substrate was a variant of a commonly manufactured grade of hand towel with a basis weight of 39gsm. The UM29 prototype was created from a lighter 29gsm paper substrate and was found to saturate with less coating than UM39 and therefore possessed a

lighter coat weight. The specifications of the UM29 and UM39 substrates are detailed in **Table 2.1**. The second component was a customized formulation of a commercially available aqueous coating VerdeCoat™ by Mantrose-Hauser, which is certified to be industrially compostable.[88]

Table 2.1. Specifications of the 29gsm and 39gsm paper substrates provided by St. Croix Tissue.

	29 gsm Substrate			39 gsm Substrate		
Attribute	Min	Target	Max	Min	Target	Max
Grammage	28	29	30	38	39	40
Thickness (microns/10 plies)	76	105	139	114	139	
Stretch (%)	5	11	18	5	11	18
Dry MD Tensile (gf/50mm, 1-ply)	3500	4150		3250	4000	
Dry CD Tensile (gf/50mm, 1-ply)	2950	3400		2600	3200	

2.2 Benchtop Fabrication Methods

2.2.1 Drawdown Coating

The drawdown method was used to apply the VerdeCoat™ functional coating to the substrate employing an RK Print Coat Instruments drawdown coating apparatus. For each test, paper substrates were prepared in a range of lengths of 150-330mm and widths of 75-200mm and weighed. In addition to the length of the sample specified for each test, 25mm was added to serve as a sacrificial lip. The addition of the lip allowed for a portion of the substrate to remain uncoated and therefore able to be easily taped to the deck of the coater while retaining the dimensions of coated sample necessary for each test. Depending on the size of the substrate and the target coat weight, 6-12mL of coating was poured into a beaker beside the coating table. On the flat drawdown bed, the substrate to be coated was placed such that the width of the paper was parallel to the coating rod. A 5mm diameter, metal, smooth coating rod was subsequently

brought to the substrate/masking tape interface, as shown in **Figure 2.1**. **Figure 2.1** displays an uncoated substrate in a drawdown coating apparatus with lines marking the cuts to be made in order to separate individual seam testing samples from the substrate once coated.

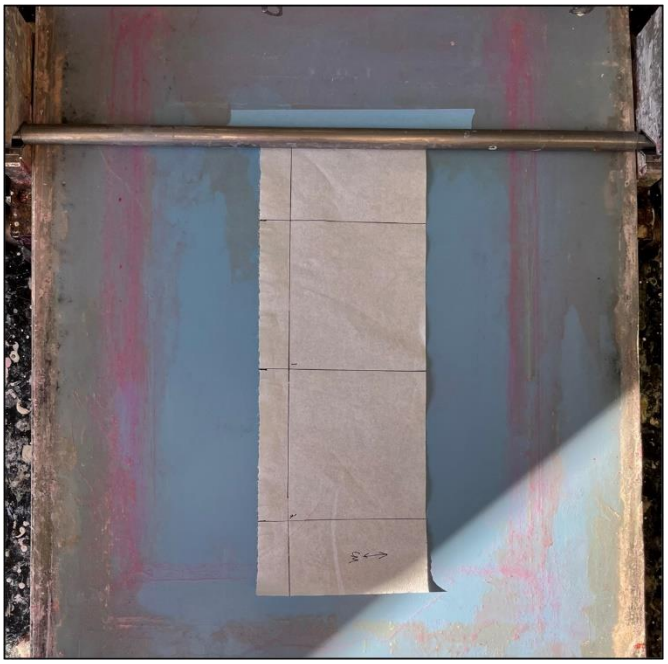

Figure 2.1. Uncoated substrate sample in the drawdown coating apparatus with the coating rod brought to the substrate/masking tape interface.

Approximately 60% of the coating in the beaker was evenly applied along the substrate/coating rod interface on the side of the rod in the direction of travel using a 10mL syringe. As the coating readily absorbed into the paper, the remaining 40% of the coating was applied linearly parallel to the coating rod at the midpoint of the substrate's length to ensure that the entire substrate was evenly coated. The coating rod was subsequently actuated down the length of the substrate at a speed of 37.5mm/s with an even force of application.

The substrate was subsequently removed from the drawdown bed by lifting the masking tape from the bed. The substrate was then attached to the ceiling of a preheated Fisherbrand™ Isotemp™ General Purpose oven via the same masking tape used to adhere the sample to the

coater bed and left to hang. The coated substrate was dried at 165°C for 3 minutes and allowed to cool for 20 minutes prior to characterization. The lip was subsequently cut using a guillotine trimmer, thereby removing the masking tape and the remaining uncoated region of the sample under the masking tape. The coated substrate was subsequently reweighed to calculate the coat weight. Once cut, the resulting product was a homogenous coated paper sample with a known coat weight. The coated paper samples were designated UM29 or UM39, as appropriate (dependent on the basis weight of the paper substrate employed). The measured coat weight of each specific sample group is reported as either UM29 or UM39 of the average coat weight ± the standard deviation of the coat weight for that group, for example, UM39 of 36 ± 2gsm.

2.2.2 Seaming Method

As isolation gowns require full protection of both the seams and the field of the material, the mechanical and barrier properties of any seams that are present must meet the same requirements as that of field material to ensure that the seam remains intact and impermeable during use. Once coated, pairs of coated samples of the same dimensions were grouped together into seaming pairs. Prior to seaming, each sample was ironed using a Rowenta DW 2192 consumer grade iron on medium heat to remove any wrinkles and to flatten the sheet. While ironing, the samples were placed under a sacrificial sheet of Unbleached Reynolds Kitchens parchment paper to prevent direct contact of the heated element with the coating surface and hence reduce the potential of heat damage. To adhere each seaming pair, both samples in the pair were placed on a flat surface covered with parchment paper. Using a 10mL syringe, a 2cm wide, straight strip of coating was deposited equally along the edge of one sample. The second sample, rotated 180° relative to the first, was placed over the coating thereby overlapping the first sample. Once again, a sacrificial piece of parchment paper was placed over the samples before

ironing along the entire length of the overlapping area on high heat. The iron was moved from one end of the overlapping area to the other, was lifted, brought to the beginning of the overlapping area, and repeatedly moved along this path five times. After removing the parchment paper, the two samples were observed to have been seamed together.

2.3 Full-sized Gown Fabrication Methods

2.3.1 Sheet Coating and Curing

In order to create a full-sized gown, a coating method that could be applied to larger sheets of substrate was investigated. The developed method consisted of rolling the coating across a sheet using a consumer-grade paint roller and subsequently curing using a heated platen press. A 4ft x 8ft metal Caul sheet was fully covered with a release sheet of ULINE S-24455 parchment paper. Subsequently, a 3ft x 6ft uncoated paper substrate was placed centrally over the parchment paper. As shown in **Figure 2.2**, the paper substrate was coated with VerdeCoat™ using a consumer-grade paint roller with a ¼" nap.

Figure 2.2. Hand roller coating of 3ft x 6ft paper substrate.

The wet, coated sheet was subsequently covered with a release layer of parchment paper and then a metal Caul sheet. The layered sample was then placed on to a 163°C heated plate and hydraulically raised to the ceiling of an Erie Mill & Press. As pictured in **Figure 2.3** the Erie Mill & Press is an automated hydraulic hot press which raises a heated platen according to instructions from a programmable logic controller.

Figure 2.3. Image of Erie Mill & Press. The heated platen plate was actuated vertically according to instructions from a programmable logic controller.

In the hot press curing protocol, the platen followed the heat/pressure/distance protocol detailed in **Table 2.2**, which approximated the benchtop coating drying method. The temperatures and heating durations followed the drawdown coating curing steps outlined in Section 2.2.1, however the use of platen plate resulted in a pressure applied to the sample, which was not applied in drawdown coating/curing.

Table 2.2. Programmed path of the heated hydraulic press. Each step was followed sequentially. The ramp time indicates the time in which the heated platen of the hot press would reach the desired position, whereas the dwell time indicates the time in which the platen would remain in the desired position. The distance and pressure attributes determined the desired position, where the heated plate would attempt to reach the designated separation distance between the platens or measure the designated 20psi of pressure exerted on the press, whichever came first.

Step	Ramp Time	Dwell Time	Distance	Pressure
1	30s	1s	0.2in	20psi
2	15s	1s	0.1in	20psi
3	15s	3min	0in	20psi

Once the programmed path of the platen press was completed, the platen was lowered from the ceiling, and the layered sample was recovered. The top metal Caul sheet layer and parchment paper layer were removed and the 3ft x 6ft sheet of coated UM39 was recovered.

2.3.2 Full-sized Gown Fabrication

Once 3ft x 6ft UM39 samples were created, a method to convert the samples into full-sized isolation gowns was developed. Two halves of a gown were excised from two 3ft x 6ft UM39 sheets using a template stencil and seamed together vertically. To create the template of an isolation gown, a commercial on-market isolation gown was obtained. The gown was cut along its seams to transition from a 3-dimensional to a planar pattern and spread out on a 6ft x 6ft sheet of paper as shown in **Figure 2.4a**. The outline, central oval-shaped head hole, and thumb holes of the gown were traced on to the paper and translated into SOLIDWORKS as shown in **Figure 2.4b**.

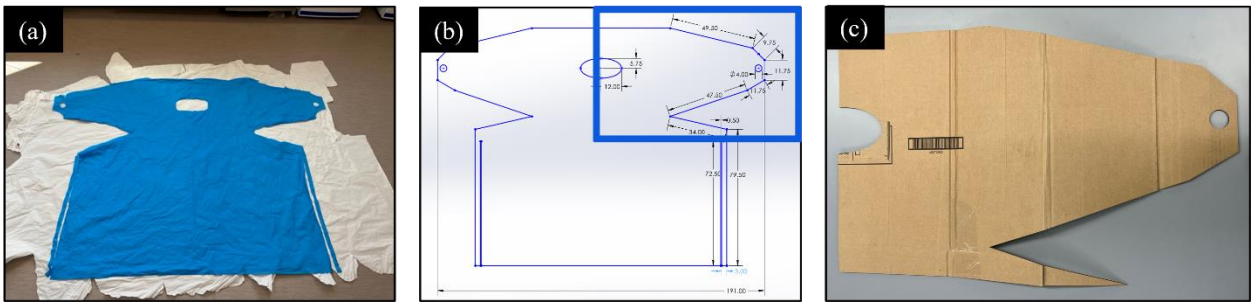

Figure 2.4. (a) Polypropylene gown traced over 6ft x 6ft sheet of paper. (b) SOLIDWORKS drawing of gown created from the measurements of the polypropylene gown with the upper right quarter highlighted. (c) Laser cut cardboard template of the highlighted upper right quarter.

From the SOLIDWORKS drawing, a Trotec Speedy 400 laser cutter was used to create a cardboard template of the drawing to use as a tracing stencil on two 3ft x 6ft UM39 sheets. As the Speedy 400 laser cutter had a maximum working area of 40in x 24in, the cardboard template was limited to the size of the upper right quarter of the drawing, indicated by the blue box in **Figure 2.4b**. Once the cardboard template, presented in **Figure 2.4c**, was fabricated, it was traced over two 3ft x 6ft sheets of UM39, exemplified in **Figure 2.5a**. The outline as well as the rectangular bottom half of the gown were excised from each sheet using a pair of consumer-grade scissors, as shown in **Figure 2.5b**.

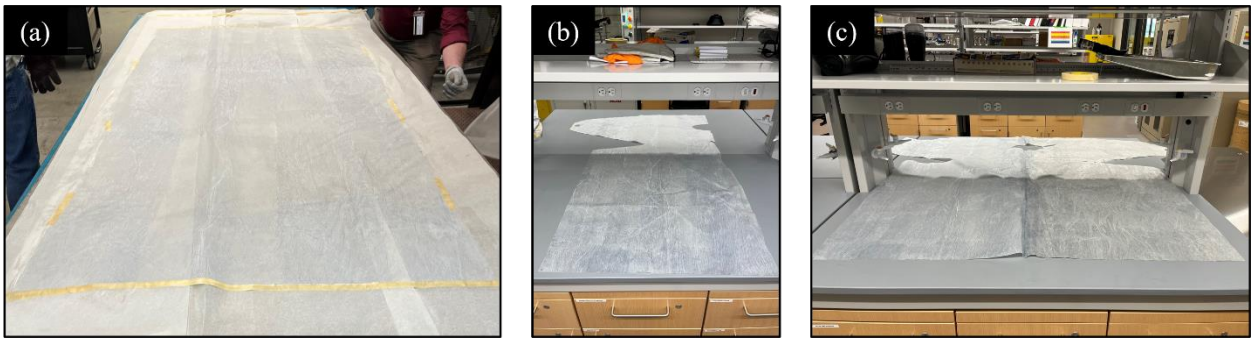

Figure 2.5. (a) 3ft x 6ft sheet of hot press coated UM39. (b) Half of a UM39 isolation gown after being excised from a UM39 sheet. (c) UM39 isolation gown made from two seamed together UM39 isolation gown halves.

Subsequently, the two halves of the gown were seamed together. To seam the two halves, the right side of the left half of the gown (shown in **Figure 2.5b**) was laid on top of a 7ft long

stretch of parchment paper. A 10mL syringe was used to deposit 30mL of VerdeCoat™ coating along the right edge of the left half of the gown. A paper towel was subsequently used to disperse the coating evenly in a 2 inch strip along the right edge of the left half of the gown. The left edge of the right half of the gown was then overlapped on top of the line of coating. The entire length of the overlapping area was then covered with parchment paper. To apply heat to seam the gown, a Rowenta DW 2192 consumer grade iron on high heat was placed on the top of the overlapping area for 10 seconds. The iron was subsequently lifted, moved 4 inches down, and placed on the overlapping area for 10 seconds. The process was repeated until the iron had traversed the entire overlapping area. Afterwards, the iron was returned to the top of the seam and forcefully moved horizontally from the outside of the overlapping area on the right side of the gown, through the seam, to the outside of the overlapping area on the left side of the gown, to ensure that the overlapping right side of the gown was fully adhered to the underlapping left side. The iron was subsequently moved 4 inches down the seam and the process repeated, until the entire length of the seam was ironed. The parchment paper over the seam was subsequently removed and the seam was observed to be well sealed except for the very bottom of the seam where the right side was slightly longer than the left. To prevent accidental peeling of one side from another due to the unevenness in lengths, a pair of scissors was used to cut a small arc approximately 2 inches in diameter into the material such that the lengths of each side were even and could not be pulled apart. The seamed gown was then hung on a coat rack to fully cure for 4 hours.

After the gown was cured, the planar gown required conversion into a 3-dimensional shape by seaming the sleeves. The top of the gown was folded along the central oval-shaped head hole, such that the top and bottom of the sleeves overlapped each other, as seen in **Figures**

2.6a and **2.6b**. The process of seaming the sleeves was identical to seaming the halves of the gown together, except that instead of seaming two separate flat sheets together, the sleeves of the gown were seamed to themselves.

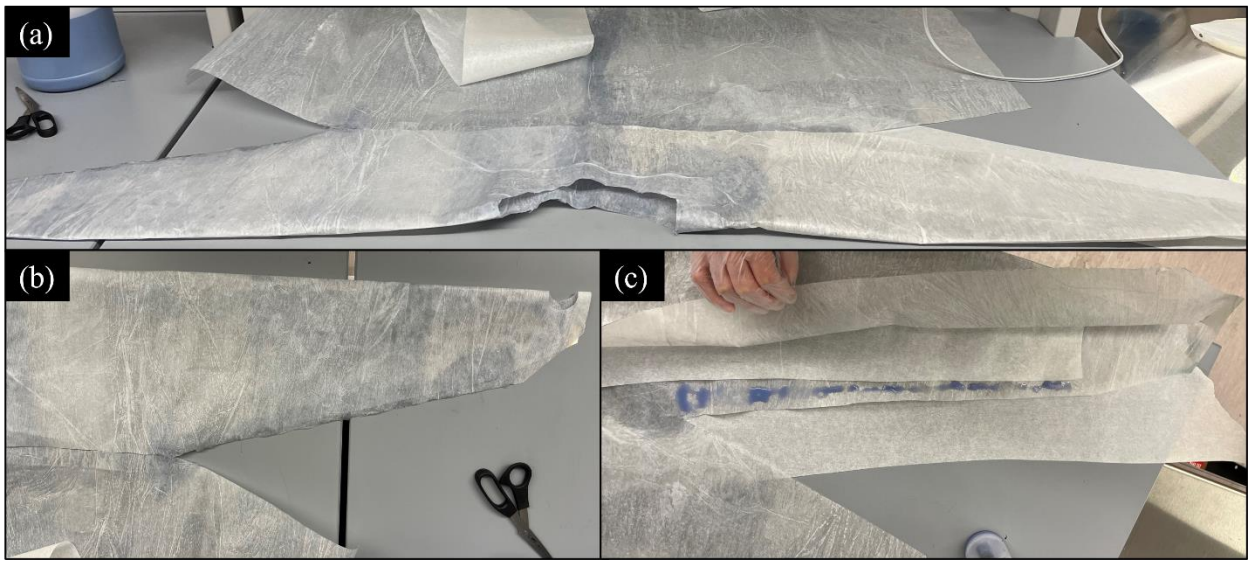

Figure 2.6. (a) Isolation gown folded about the central head hole. (b) Overlayed top and bottom of isolation gown sleeve. (c) Application of coating to the isolation gown sleeve with an intermediary parchment paper layer to prevent seaming inside the sleeve.

Once overlapped, a piece of parchment paper was inserted inside the sleeve to prevent the space interior to the seam from becoming sealed. As shown in **Figure 2.6c**, a line of coating was subsequently applied to the approximately 1.5-inch edge of the sleeve and heat sealed as previously described.

2.4 F3352 Test Methods

2.4.1 AATCC 42 Impact Penetration Test

The American Association for Textile Chemists and Colorists (AATCC) 42 Impact Penetration Test is used to determine the impact penetration resistance (IPR) of a textile material to water. The IPR of a material is determined by the ability of the material to resist the penetration of water showered upon it, which mimics accidental fluid spraying in hospital settings. The following procedure was derived from the AATCC 42 test method.[89] Four sample groups were evaluated: an on-market AAMI Level 3 polypropylene gown, UM29 of 16 ± 1gsm, UM39 of 37 ± 5gsm, and UM39 seam of 36 ± 2gsm coat weight. For each sample group, three 178mm x 330mm samples were prepared. For each sample, a 152 x 230mm piece of 249.21gsm Ahlstrom Munksjö MHPM0240 blotter paper was cut and weighed. Upon testing, a single sample covered a single piece of blotter paper and was held in placed using a board clip. The clipboard was then placed 0.6m under the testing apparatus at an angle of 45° as shown in **Figure 2.7**.

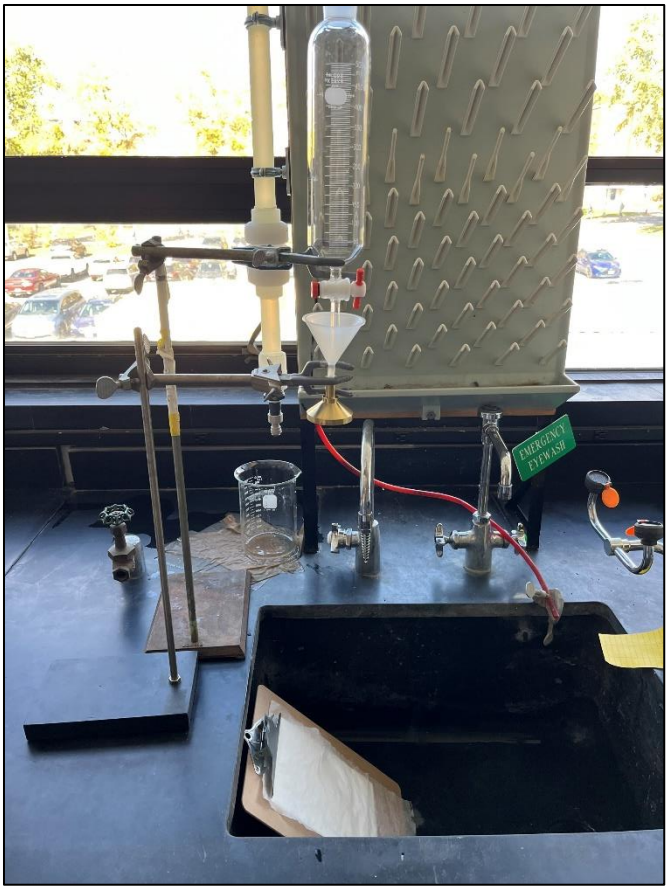

Figure 2.7. Impact Penetration Testing Apparatus made from a Separatory Funnel, Plastic Funnel, Impact Penetration Head, and Ring Stands.

The apparatus consisted of a 500mL glass separatory funnel suspended above a plastic funnel via a ring stand and clamp. The plastic funnel rested upon the inlet of an 78384A AATCC Impact Penetration Head (IPH) that was suspended by another ring stand and clamp. The IPH was a machined bronze shower head purchased from the AATCC with specific hole spacings and diameters detailed in **Appendix A.2**. To begin the test, 500mL of deionized water was poured into the separatory funnel and the stopcock was released, allowing the water to pour out of the separatory funnel, into the plastic funnel, through the IPH, and shower on to the sample which covered the blotter paper. Once flow from the IPH ceased, the blotter paper was quickly removed from the clipboard and immediately weighed. The difference in the mass of the blotter paper pre

and post test indicated the mass of the water which penetrated through the sample and was taken up by the blotter paper.

2.4.2 AATCC 127 Hydrostatic Pressure Test

The AATCC 127 Hydrostatic Pressure Test measures a material's ability to resist water penetration from a static pressurized source. The AATCC 127 test is a more rigorous determination of resistance to water penetration than the AATCC 42 test and is used to characterize Class 2 and 3 isolation gowns. The following procedure was derived from the AATCC 127 test method.[90] Four sample groups were evaluated: an on-market AAMI Level 3 polypropylene gown, UM29 of 19 ± 1gsm, UM39 of 32 ± 1gsm, and UM39 seam of 32 ± 2gsm coat weight. For each sample group, three 200mm x 200mm samples were prepared. As the samples were too porous for air-actuated hydrostatic pressure tests, an OT-MLLCR-2314 Textile Fabric Hydrostatic Pressure Tester from CNCEST was modified to create hydrostatic head pressure using a column of water. As seen in **Figure 2.8**, the device was constructed with an open-ended U-shaped tube which could be filled with deionized water. The 90cm long tube had an inner diameter of 3/8in and outer diameter of 1/2in. The ends of the U-shaped tube were termed the inlet and outlet. The inlet was attached via a hose clamp to, and suspended by, a plastic funnel resting on a ring stand. A yardstick was placed perpendicularly to the funnel to measure the height of the rim of the funnel relative to the base of the ring stand. The outlet of the U-shaped tube was connected to a hydrostatic pressure tester (HPT). The HPT was originally designed for air-actuated hydrostatic pressure testing and was modified to instead accept a flow of water. The HPT consisted of two components: the reservoir and the clamp. The reservoir was a hollow cylindrical container with a circular hole at its top and an inlet at its base. Above the

reservoir, a screw clamp was centered and could be turned to press a sample against the periphery of the reservoir hole.

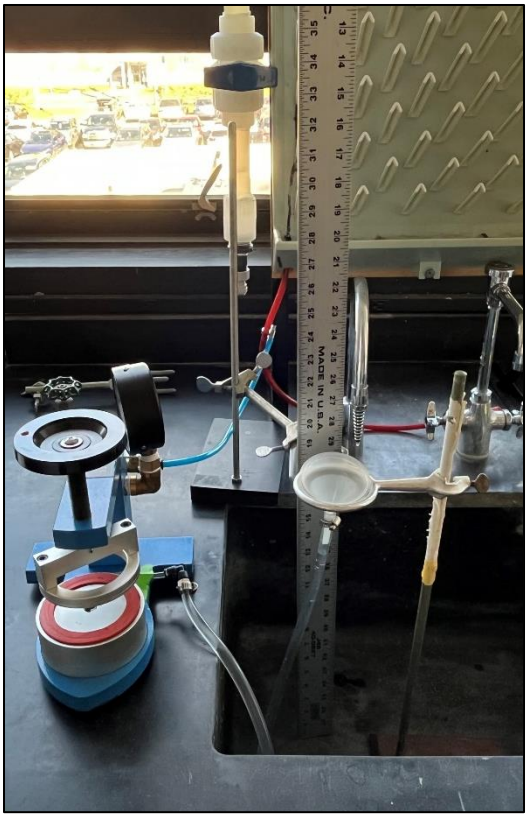

Figure 2.8. Hydrostatic Pressure Testing Apparatus. Head Pressure based Testing System composed of a U-shaped tube with inlet (right) and outlet (left) connected to an OT-MLLCR-2314 Hydrostatic Pressure Tester.

To begin the test, the HTP was primed with deionized water via the inlet until the reservoir inside the HPT was full and deionized water was pushed through the circular hole at the top of the reservoir. Once the deionized water reached the top of the hole, a sample was centered over the hole and clamped with its coated side down using the circular screw clamp. By clamping the sample, deionized water was prevented from leaving the hole centered under the coated paper. Once such configured, the height of the deionized water at the top of the hole was equal to the height of deionized water on the inlet side of the U-shaped tube. The funnel was subsequently manually raised at a rate of approximately 1 centimeter per second and the clamped

sample was monitored for signs of water penetration. The height differential between the water levels of the inlet and outlet created a hydrostatic head pressure on the sample. Once three beads of water appeared on the non-coated side of the sample, the test was terminated and the height of the rim of the funnel at which the beads penetrated the sample was recorded. The difference in the starting height and the ending height determined the hydrostatic failure pressure in units of cmH_2O.

2.4.3 ASTM D5034 Grab Test

The ASTM D5034 Grab Test measures a material's tensile strength, which is defined as the maximum amount of tensile force necessary to break the material. Isolation gowns are subjected to the D5034 test to determine their ability to maintain integrity under mechanical stresses. The following procedure was derived from the ASTM 5034 test method.[91] Three sample groups were evaluated: an on-market AAMI Level 3 polypropylene gown, the uncoated 39gsm paper substrate, and UM39 of 37 ± 3gsm coat weight. For each sample group, five 195mm x 100mm and five 100mm x 195mm samples were prepared. Reciprocal dimensions of the samples were cut to test both the machine and cross machine tensile strengths of the samples. All samples were conditioned at 23°C and 50% relative humidity in the TAPPI room of the Process Development Center (PDC) at the University of Maine for at least 12 hours prior to testing. A 2kN capacity Instron model 5564 was used to test the tensile strength of each sample. The two jaws on the Instron each had a jaw face of 25mm x 25mm and were aligned horizontally but spaced 75mm apart vertically along the direction of applied tensile force. The jaw faces were lined with aluminum oxide 180 grit sandpaper for increased traction on the sample. When loaded, each sample was placed between the jaws with its longer side vertically such that the horizontal midpoints of the jaws and the sample overlapped. Similarly, the vertical midpoint of

the sample was brought to the center of the distance between the jaws. With the sample pneumatically clamped in position by both jaws, the top jaw was raised at a rate of 300mm per minute and the extension as well as the force required to maintain the constant rate of extension were recorded by the Instron.

2.4.4 ASTM D5733 Tear Test

The ASTM D5733 Tear Test measures the ability of a material to resist the propagation of a tear through itself. The following procedure was derived from the ASTM D5733 test method.[92] Three sample groups were evaluated: an on-market AAMI Level 3 polypropylene gown, the uncoated 39gsm paper substrate, and UM39 of 36 ± 4gsm coat weight. For each sample group, five 150mm x 75mm and five 75mm x 150mm samples were prepared. Reciprocal dimensions of the samples were cut to test both the machine and cross machine tensile strengths of the samples. A slit 15mm long was cut orthogonally into the sample from the midpoint of the longer side using a pair of scissors. The samples were conditioned at 23°C and 50% relative humidity in the TAPPI room of the PDC at the University of Maine for at least 12 hours prior to testing. An Instron model 5564 was used to test the tear strength of each sample. The two jaws on the Instron each had a jaw face of 25mm x 25mm and were aligned horizontally but spaced 75mm apart vertically along the direction of applied tensile force. The jaw faces were lined with aluminum oxide 180 grit sandpaper for increased traction on the sample. When loaded, each sample was placed between the jaws with its longer side vertically such that the horizontal midpoints of the jaws and the sample overlapped, as seen in **Figure 2.9**. Similarly, the vertical midpoint of the sample was brought to the center of the distance between the jaws. With the sample pneumatically clamped in position by both jaws, the top jaw was raised at a rate of 300mm per minute and the extension as well as the force required to maintain the constant rate

of extension were recorded by the Instron. Failure was defined as the force required to propagate the tear to sample separation.

Figure 2.9. ASTM D5733 Test sample mounted in an Instron model 5564.

2.4.5 ASTM D1683 Seam Test

The ASTM D1683 Seam Test measures the force required to break a seam connecting two pieces of material. As isolation gowns require full protection throughout the entire gown, the tensile strength of the seam must meet the same strength requirement as that of continuous material to ensure that the seam remains sealed during use. The following procedure was derived from the ASTM D1683 test method.[93] Two sample groups were evaluated: an on-market AAMI Level 3 polypropylene gown and a UM39 seam of 29 ± 2gsm coat weight. For each sample group, five 200mm x 100mm and five 100mm x 20mm samples were prepared. The UM39 seam samples were fabricated as detailed in Section 2.2.3. The samples were subsequently conditioned and tested in the same manner as outlined in the ASTM 5034 Grab Test.

2.4.6 Statistical Analysis of F3352 Test Methods

After conducting the ASTM F3352 dictated test methods for groups of uncoated and coated paper samples, as well as the Level 3 polypropylene gown, JMP Pro software was used to perform a one-way ANOVA test to determine the presence of a statistically significant difference between groups ($\alpha < 0.05$). Once the ANOVA test determined a statistically significant difference, a Tukey Honestly Significant Difference (HSD) Test was performed to determine which groups were significantly different from each other ($\alpha < 0.05$). Statistically significant differences are shown by a connecting letters representation, in which groups annotated by different letters are statistically different.

2.5 Contact Angle Testing

Sessile drop contact angle testing was performed on on-market AAMI Level 3 polypropylene gown and UM39 samples created via different fabrication and post-processing methods in order to quantify UM39's degree of hydrophobicity. A single sample was chosen from each group of materials of similar fabrication methods. Three deionized water droplets were deposited on each sample using a 1mL syringe. A cross-sectional image of each droplet was taken using an iPhone 13 with default settings. On each image, the sample's surface and a tangent of the edge of the droplet's shape were identified and marked with red lines. As shown in **Figure 2.10**, the resulting angle between the red lines on the interior side of the droplet was measured to determine the sessile drop contact angle of the sample.

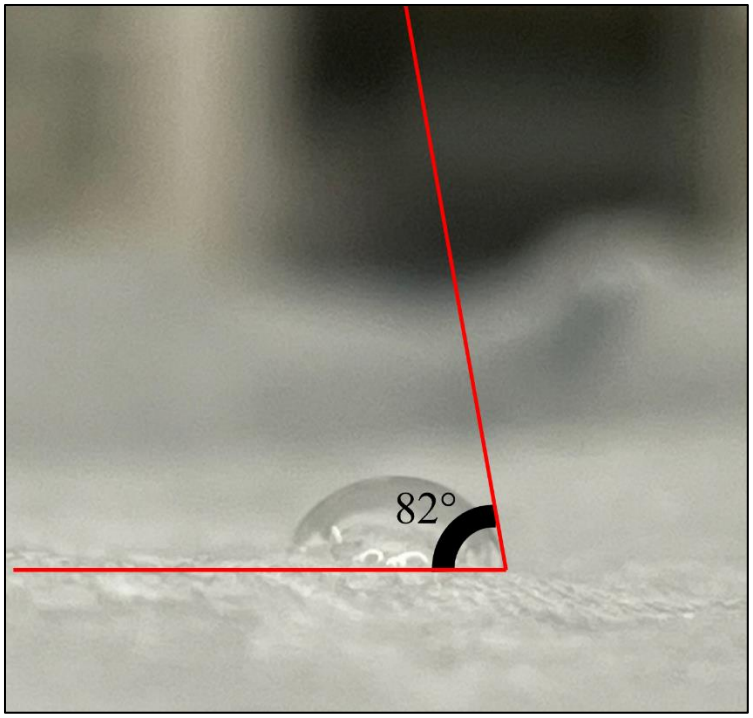

Figure 2.10. Water droplet on a UM39 sample. The red lines indicate the sample's surface and tangent line of the edge of the droplet used to determine the contact angle. The angle of the intersection of the red lines is displayed.

2.6 Composting Trials

2.6.1 Initial Ranging Study

In order to test the compostability of UM39, an industrial composting study was designed in partnership with Casella Organics Hawk Ridge in Unity, Maine. For the compostability study, UM39 and uncoated substrate samples were placed in a windrow and monitored for degradation over time via loss of mass, bypassing the active composting phase. The active composting stage of the industrial process was bypassed due to the infeasibility and safety concerns of tracking a sample through the Dutch Tunnel process. As such, the windrow experiment models 'worst-case' degradation as it omits the most active phase of sample degradation. By bypassing the high-

microbial composting phase, the samples were exposed to less microbial activity than would otherwise be expected by a material undergoing the entire industrial process. Thus, a material that degraded under the 'worst-case' scenario would be expected to degrade at least as quickly with the integration of the active composting phase. The metric of dry mass loss over time was determined to be the best method to track the degradation of the samples due to the measurement's independence of moisture content or shape of the sample, which would both change over time in the windrow.

The following procedure was devised: 11cm x 11cm samples of UM39 of 31 ± 1gsm coat weight and its uncoated substrate were created, oven dried at 105°C for 30 minutes, and weighed to determine their initial dry weight. A drying time of 30 minutes was determined to be sufficient to reach the dry weight of the samples from a drying test. Specifically, four UM39 samples were fully immersed in deionized water for a period of one hour and subsequently weighed. The samples were then placed in an oven at 105°C and weighed over a period of 22 hours. **Figure 2.11** displays a plot of the samples' mass against drying time.

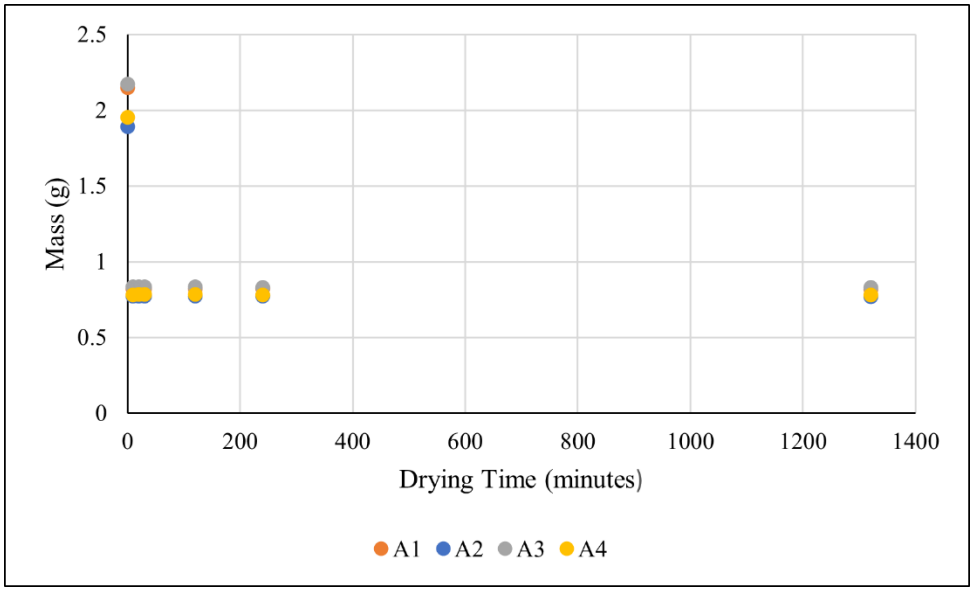

Figure 2.11. Mass of initially wet UM39 samples after a period of drying at 105°C for up to 22 hours. Mass measurements at time t=0 were taken prior to any drying.

Analysis of **Figure 2.11** demonstrates an overall trend of the initially wet UM39 samples of approximately 2g rapidly decreasing in mass to 0.75g in 30 minutes of drying with no noticeable difference in mass between oven drying for 30 minutes and 22 hours. Furthermore, the average difference in mass between these two time points was determined to be 0.004 ± 0.002g. Due to the negligible difference in mass, 30 minutes of drying was determined to be sufficient to reach the dry mass of the UM39 samples.

In addition to the 11cm x 11cm samples, 2cm x 21cm UM39 samples were created and evaluated to model samples with a geometry that may arise from the shredding of the material before composting. The weighed samples were subsequently placed in red Nylon SRXES B08FWYVH9X mesh onion bags for visibility and containment once placed in the windrow. Twelve equidistant points along one side of a given windrow were marked with wooden stakes to identify sample locations and enable later retrieval. The points were numbered sequentially from one end of the windrow to the other. At each point along the windrow, a Nylon bag

containing an uncoated substrate sample and a Nylon bag containing a UM39 sample were inserted into the windrow. The samples were inserted approximately 36” inwards horizontally from the edge of the windrow and 18” or 24” vertically down from the height of the windrow at that designated horizontal distance for uncoated and UM39 samples, respectively. A diagram of the placement of the UM39 samples is presented in **Figure 2.12**, where the light brown triangle represents a single side of a windrow and the dark brown trapezoid indicates the hole in which the UM39 samples were inserted prior to being filled in.

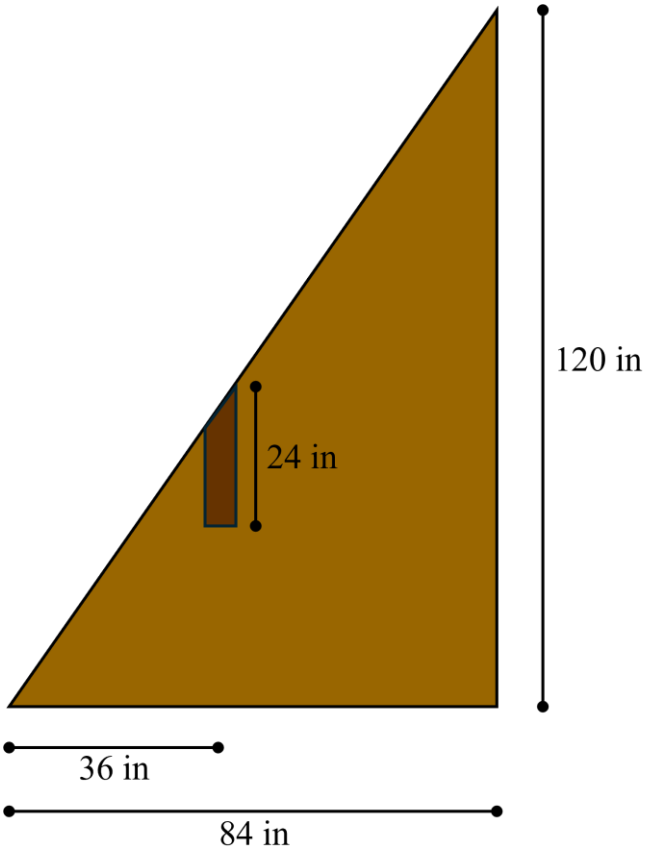

Figure 2.12. Diagram of UM39 sample placement inside of a windrow. The UM39 samples were placed 24” vertically downward from the height of the windrow 36” horizontally from its edge.

The samples were divided into four groups based on the sequential number of the point in which they were inserted. The first group was comprised of the first, fifth, and ninth points, with subsequent groups comprised of n, n+4, and n+8 points for n=2,3,4. After three days in the windrow, the three samples of the first group were removed from the windrow and extracted from the Nylon mesh bag. The samples were subsequently dusted using a Fisherbrand™ General-Purpose Laboratory Brush 03-645A, weighed, photographed, oven dried at 105°C for 30 minutes in a Fisherbrand™ Isotemp™ General Purpose oven, and reweighed. To ensure the samples were not dislodged from their placement position in the oven by the convection fan when drying, each sample was placed on a parchment paper covered oven rack under an inverted 100mL beaker. For a given sample, the proportion of the sample's measured dry weight post-composting relative to its original dry weight was reported as its extent of degradation at the relevant timepoint. The remaining samples in the windrow were evaluated in triplicate in the same manner after 7, 24, and 52 days in the windrow. The samples remained in the windrow for the duration of the study until they were removed with the exception of temporary removal and replacement during periodic windrow turning. The process of windrow turning was undertaken in order for the facility to maintain and reinvigorate microbial activity and entailed a bucket loader lifting and dropping the compost material in the windrow to induce mixing. Prior to turning, all samples were removed from the windrow and placed in plastic bags for approximately one hour while the windrow was turned. Once the windrow turning was complete, the samples were reinserted in their original location in the windrow. In the initial ranging study, the windrow was turned on days 10, 29, and 43. Furthermore, at time points over the course of the study, a CompostManager probe was inserted perpendicularly approximately 1ft to the right of each wooden stake and 2ft deep into the window. The probe was employed to measure the

temperature, oxygen concentration, carbon dioxide concentration, and moisture content of each point in the windrow, which served as data input for windrow management and determination of the optimal time for turning.

2.6.2 Extended Duration Study

Based on the findings of the ranging study and the subsequent obtainment of the ASTM 6868 standard, an extended composting study was designed and conducted. The ASTM 6868 Standard Specification for Labeling of End Items that Incorporate Plastics and Polymers as Coatings or Additives with Paper and Other Substrates Designed to be Aerobically Composted in Municipal or Industrial Facilities outlines a number of tests that must be conducted to label a product as industrially compostable.[94] The primary test is the ISO 16929 Plastics - Determination of the degree of disintegration of plastic materials under defined composting conditions in a pilot-scale test.[95] While the ISO 16929 test method traditionally requires a laboratory test, the determination was made to incorporate multiple elements of the test into an extended industrial composting study to more accurately model the ISO 16929 standard. In the extended study, any non-explicitly mentioned methods employed in the original Ranging Study experimental protocol were preserved.

Twelve 5cm x 5cm samples of UM39 of 30 ± 4gsm coat weight and the uncoated substrate were prepared and inserted into the windrow in the same manner outlined in the Ranging Study. As in the Ranging Study, the samples of the twelve marked locations were divided into four groups, comprised of n, n+4, and n+8 samples for n=1,2,3,4. As presented in **Figure 2.13**, the samples were removed from the windrow after 21*n days for n=1,2,3,4 where n denoted the sample's group number.

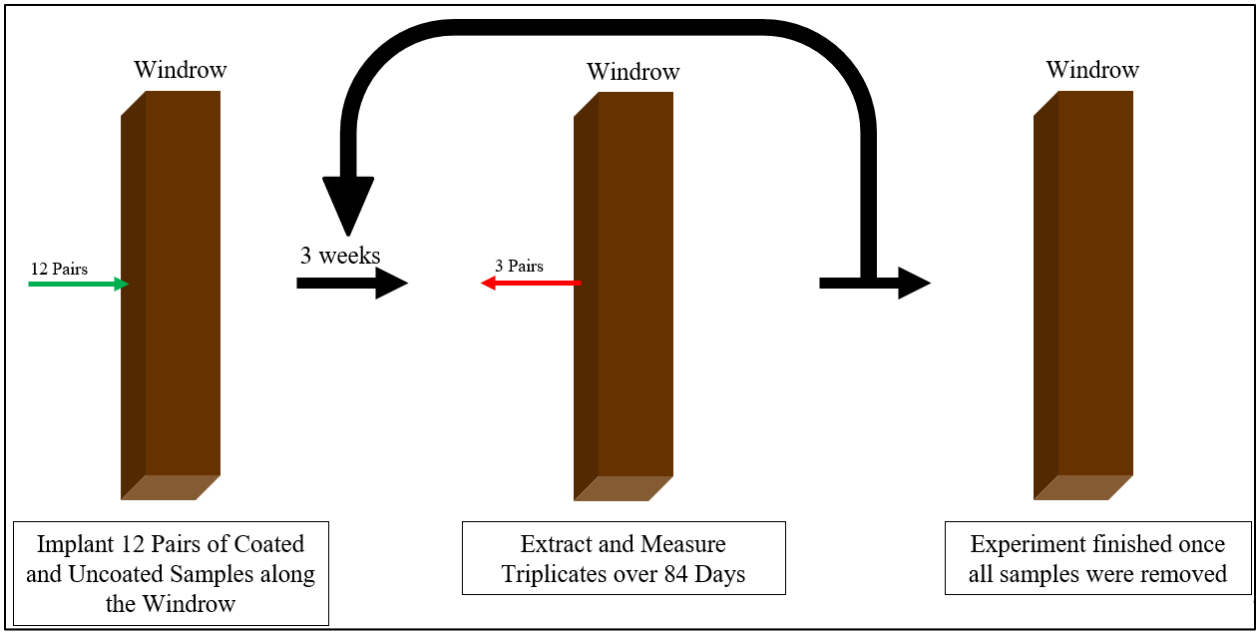

Figure 2.13. Diagram of the removal procedure of the extended duration composting study samples. Three UM39 and uncoated substrate control samples pairs were removed from the windrow at 21-day intervals over a period over 84 days.

The samples remained in the windrow until they were removed except for turning which occurred on days 14, 35, and 70; the same removal and replacement protocol as employed for the Ranging Study was employed for the Extended Study. Once removed from the windrow and extracted from the Nylon mesh bag, samples were sieved through a 10mm screen and a 2mm screen (Global Gilson V200SF series), and subsequently weighed, photographed, oven dried at 105°C for 30 minutes, prior to being reweighed.

CHAPTER THREE: Standardized Testing Results

3.1 F3352 Test Methods for Drawdown Coated Samples

3.1.1 AATCC 42 Impact Penetration Test

The AATCC 42 Water Resistance: Impact Penetration Test (AATCC 42), originally envisioned to predict the resistance of a fabric to outdoor precipitation, is used in the F3352 standard to predict the resistance of a gown to accidental exposure of fluid spray in a hospital setting. In accordance with the AATCC 42 standard, a test sample was placed over an absorbent piece of blotter paper and rained upon in the method outlined in Section 2.4.1. For PB70 Level 3 barrier protection classification, which is the greatest level of protection attributable by this test, less than 1g of water is allowed to penetrate the sample and be absorbed by the blotter paper. **Figure 3.1** presents a plot of specimen vs mass of water penetration for an on-market AAMI Level 3 polypropylene gown, the UM29 prototype of 16 ± 1gsm, the UM39 prototype of 37 ± 5gsm, and the seam of the UM39 prototype of 36 ± 2gsm coat weight.

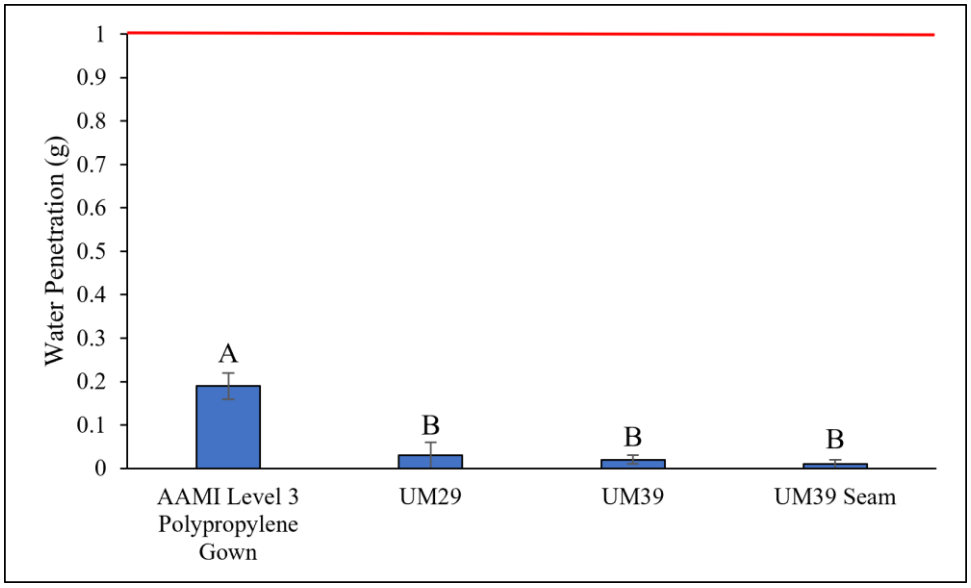

Figure 3.1. AATCC 42 Impact Penetration Testing Results of the polypropylene gown, UM29, UM39, and UM39 seam materials with the maximum allowed water penetration for Level 3 classification denoted by the red line. Statistical differences are designated by differing letter annotations.

Analysis of the data in **Figure 3.1** demonstrates that while all tested samples were below the threshold value for Level 3 classification and therefore passed the test, the overall trend indicates that the impact penetration for the polypropylene gown was the greatest, followed by the UM29 and then the UM39 samples. The UM29, UM39, and UM39 Seam samples were all statistically equivalent, but statistically lower than the polypropylene sample. As such, the coated paper materials demonstrated superior barrier performance compared to the on-market conventional polypropylene gown. Furthermore, the UM39 Seam sample performed equivalently to the continuous material. Therefore, it is evident that the seaming method of heat sealing produces similar barrier properties to that of the continuous material.

3.1.2 AATCC 127 Hydrostatic Pressure Test

The AATCC 127 Water Resistance: Hydrostatic Pressure Test (AATCC 127) measures the resistance of a material to the penetration of water under hydrostatic pressure. In a clinical

setting, a material's resistance to hydrostatic pressure can be representative of its resistance to the penetration of the material from pressurized sources such as the circulatory system. For each AATCC 127 test, one side of a tested sample experienced increasing hydrostatic pressure until three points of liquid penetration were seen on the opposite side of the sample, as detailed in Section 2.4.2. The sample must meet or exceed a pressure threshold of 50 cmH_2O to qualify for PB70 Level Class 3 protection under the AATCC 127 test. **Figure 3.2** presents a plot of specimen vs hydrostatic failure pressure for an on-market AAMI Level 3 polypropylene gown, the UM29 prototype, the UM39 prototype, and the seam of the UM39 prototype.

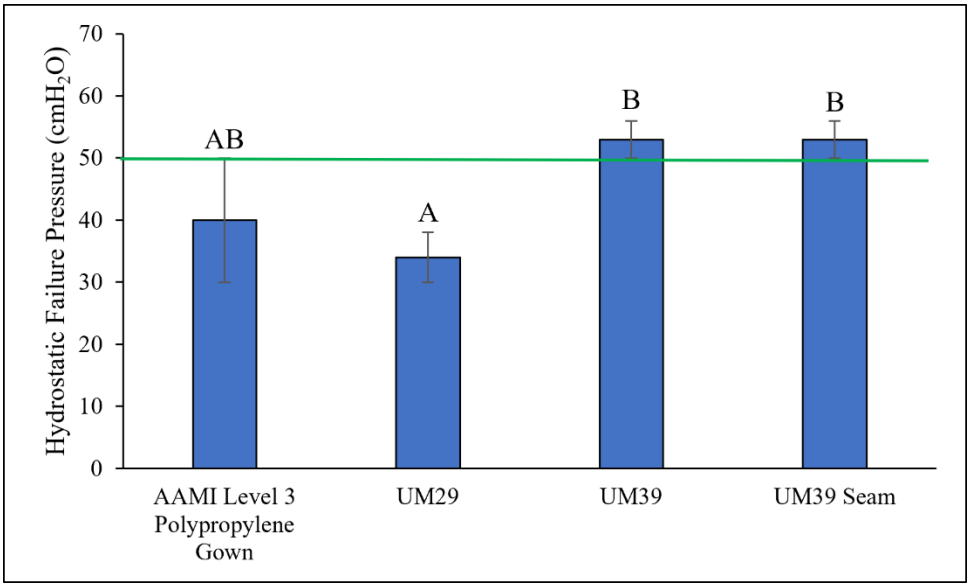

Figure 3.2. AATCC 127 Hydrostatic Pressure Testing Results of the polypropylene gown, UM29, UM39, and UM39 seam materials with the minimum allowable failure pressure for Level 3 classification denoted by the green line. Statistical differences are designated by differing letter annotations.

Analysis of the data in **Figure 3.2** demonstrates an overall trend of the UM39 continuous and seamed material having the greatest hydrostatic pressure resistance, followed sequentially by the on-market polypropylene gown, and then the UM29 material. The UM39 field and seamed material both resisted 53 ± 3 cmH_2O of pressure before penetration, exceeding the 50 cmH_2O

threshold for PB70 Level 3 classification, while the UM29 material only resisted 34 ± 4 cmH_2O, which classified UM29 as PB70 Level 2. Similarly, the polypropylene gown resisted 40 ± 10 cmH_2O before water penetration. While the on-market polypropylene gown was not found to be statistically different from the UM29 or UM39 material, the UM39 and UM29 materials were found to be statistically different from each other. As stated in Section 2.4.2, the coat weight of the UM29 samples averaged 19 ± 1gsm while the UM39 samples averaged 32 ± 1gsm. It is hypothesized that the UM39 material resisted a greater hydrostatic pressure than the UM29 material since the increased basis weight of the 39gsm substrate allowed for more coating to be absorbed into the material compared to the 29gsm substrate. Although the UM29 prototype was preferred due to its decreased basis weight, which would lead to a more lightweight and potentially more pliable and better draping gown, the performance difference of the UM29 and UM39 materials in the AATCC 127 test led to the determination that the UM39 prototype was the better candidate from which to construct compostable isolation gowns. The determination was strengthened by the results of multiple studies demonstrating that commonly used Level 1 and 2 isolation gowns may not provide adequate barrier properties.[41,42] Therefore, further testing (i.e. of physical properties) was not performed on the coated UM29 material.

3.1.3 ASTM D5034 Grab Test

The ASTM D5034 Standard Test Method for Breaking Strength and Elongation of Textile Grab Test provides a standardized measurement of the ultimate tensile force required to break a material. As the degree of force required to tear apart a material is dependent on a number of factors such as the cross-sectional area that the force is applied to, as well as the orientation and conditioning of a sample, the D5034 test serves as a method to standardize the measurement of the breaking strength of a material. The breaking strength itself is defined as the

force at which a tested sample is broken apart and is represented by the peak force recorded in a load-extension curve resulting from a standardized tensile test, as detailed in Section 2.4.3. The F3352 standard requires the breaking strength of the prototype material to exceed 30N. **Figure 3.3** presents a plot of specimen vs tensile strength for the machine direction (MD) and cross-machine direction (CM) of an on-market AAMI Level 3 polypropylene gown and the coated UM39 prototype of 37 ± 3gsm coat weight. The tensile strength of the uncoated 39gsm substrate is also shown to elucidate the impact of coating on the substrates' tensile strength.

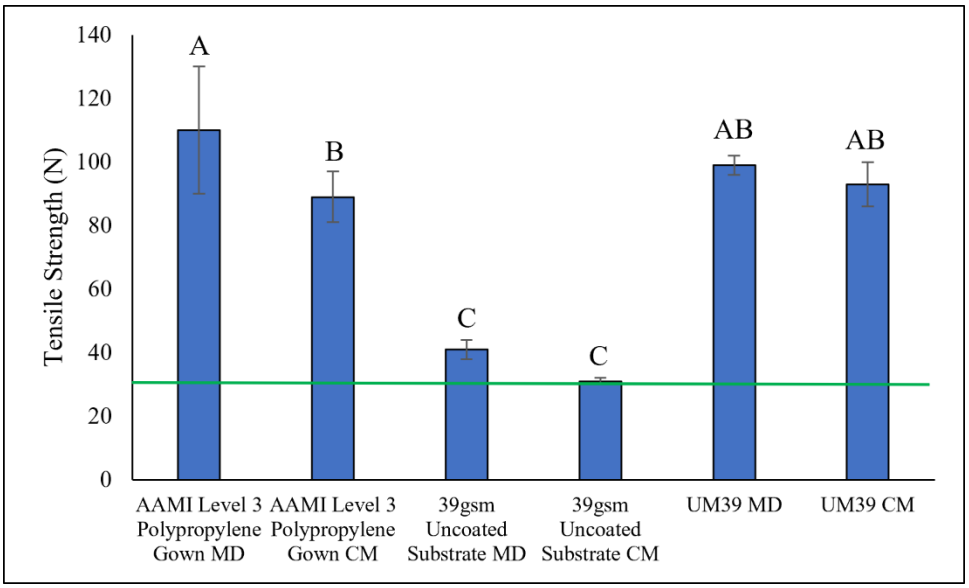

Figure 3.3. ASTM D5034 Grab Testing Results of the polypropylene gown, UM29, UM39, and UM39 seam materials with the minimum allowable breaking strength denoted by the green line. Statistical differences are designated by differing letter annotations.

Analysis of **Figure 3.3** indicates that all samples exceeded the 30N threshold requirement of the F3352 standard. The overall trend demonstrates that the MD polypropylene material possessed the greatest tensile strength, followed sequentially by both directions of the UM39, the CM polypropylene, and lastly both directions of the uncoated substrate. The UM39 and

polypropylene materials were found to be statistically similar, therefore implying that UM39 material possesses similar tensile strength to on-market isolation gowns.

Furthermore, upon coating, the tensile strengths of the 39gsm uncoated substrates were found to greatly increase from 41 ± 3N and 31.0 ± 0.7N for MD and CM, respectively, to 99 ± 3N and 93 ± 7N for MD and CM UM39, respectively. As such, the UM39 material performed similarly to an on-market gown material and far surpassed the ASTM F3352 requirement.

3.1.4 ASTM D5733 Tear Test

The ASTM D5733 Standard Test Method for Tearing Strength of Nonwoven Fabrics by the Trapezoid Procedure measures a material's ability to resist the propagation of an existing tear. The Tear Test serves as a secondary measure of protection to ensure that if a tear in the material does occur, the remaining continuous fabric of the gown would not significantly rupture due to the application of a given amount of force. The D5733 test models this scenario by determining the breaking strength of a sample with a premade cut, henceforth referred to as the material's tear strength; see Section 2.4.4 for the experimental protocol. To meet the requirements of the F3352 standard, the tear strength of the tested material must be greater than 10N. **Figure 3.4** presents a plot of specimen vs tear strength for the MD and CM of an on-market AAMI Level 3 polypropylene gown, the uncoated 39gsm substrate, and the coated UM39 prototype of 36 ± 4gsm coat weight.

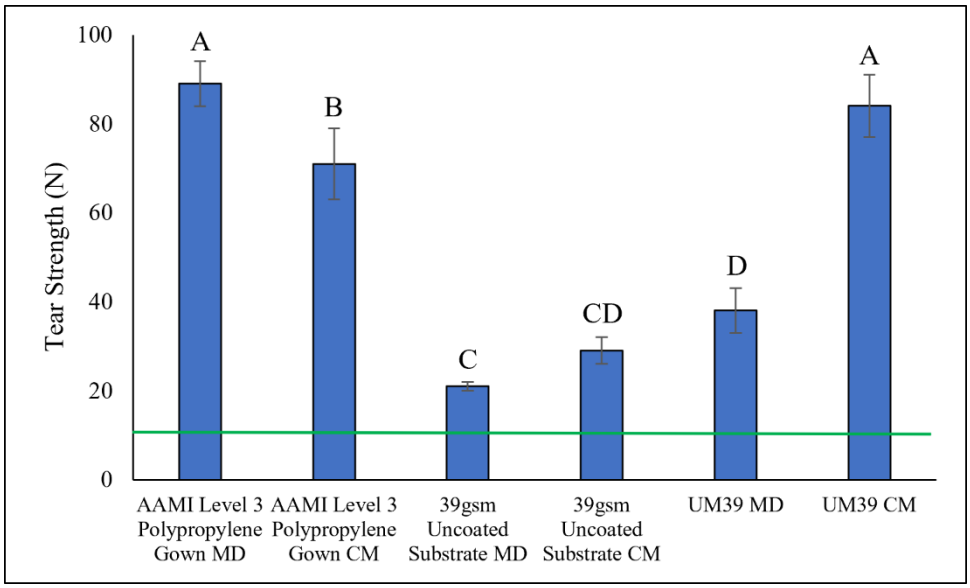

Figure 3.4. ASTM D5733 Tear Testing Results with the minimum allowable tear strength denoted by a green line. Statistical differences are designated by differing letter annotations.

Analysis of **Figure 3.4** indicates that all samples exceeded the threshold value of 10N and therefore met the standard. The material with the greatest tear strength was the MD polypropylene, followed sequentially by the CM UM39, CM polypropylene, MD UM39, CM uncoated substrate, and MD uncoated substrate. The performance of the CM UM39 samples was statistically equivalent to that of MD polypropylene samples, however the tensile strength of the MD UM39 samples, while nearly four times exceeding the D5733 strength requirement, was approximately half that of the CM UM39 samples and performed statistically worse than either of the polypropylene directions. It is hypothesized that the weaker MD is due to the directionality of the cellulosic fibers of the substrate. Specifically, as the fibers are aligned along the MD, severing these fibers in the MD D5733 test weakens the cellulosic structure of the sample more than cutting parallel to the fibers.

Furthermore, coating the paper substrate caused a statistically significant increase in tear strength. The uncoated 39gsm paper substrate recorded a MD and CM tear strength of 21 ± 1N

and 29 ± 3N, respectively, whereas the coated material recorded a tear strength of 38 ± 5N and 84 ± 7N for MD and CM, respectively. It is evident that, as seen for the tensile test results, coating the substrate greatly increased its strength. However, unlike the tensile test, the CM strength was greater than the MD strength. The discrepancy may be explained by the location of the initiation of breakage in the samples. In experimental trials, the MD samples were found to initiate their tear along the premade cut, whereas the initiation of the tear of the CM samples did not necessarily coincide with the location of the cut but instead initiated from unpredictable locations. However, the unpredictability of the initiation locations of the tear test samples was consistent with the tensile test samples and may indicate that the tear strength of the CM UM39 may be greater than, or similar to, its tensile strength.

3.1.5 ASTM D1683 Seam Test

The ASTM D1683 Standard Test Method for Failure in Sewn Seams of Woven Fabrics measures the breaking strength of a seam connecting two pieces of continuous material. As seams are necessary in order to convert industrially produced flat material sheets into three-dimensional isolation gowns, the D1683 test is used to ensure that the seams meet the same physical property threshold requirements as the continuous material; see Section 2.4.5 for the experimental protocol. **Figure 3.5** presents a plot of specimen vs seam strength for MD and CM UM39 of 29 ± 2gsm coat weight and an on-market AAMI Level 3 polypropylene gown.

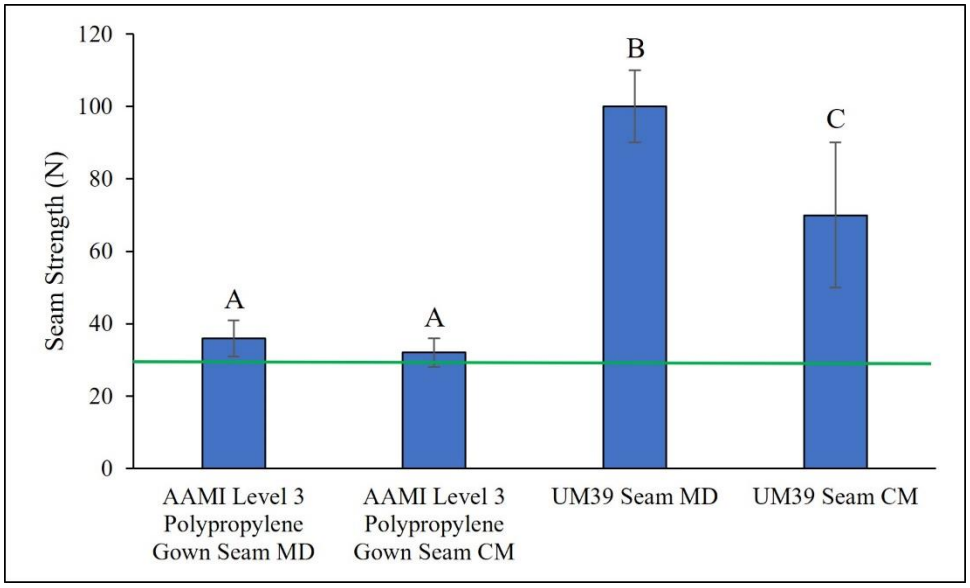

Figure 3.5. ASTM D1683 Seam Testing Results of the polypropylene gown and UM39 seam materials with the minimum allowable seam strength denoted by the green line. Statistical differences are designated by differing letter annotations.

Analysis of **Figure 3.5** demonstrates that while all samples exceeded the 30N threshold requirement, the breaking strength of the seamed UM39 material, referred to as its seam strength, was much greater than that of the polypropylene gown. The seam strength of UM39 was 100 ± 10N and 70 ± 20N for MD and CM UM39, respectively, whereas the seam strength of the AAMI Level 3 polypropylene gown was 36 ± 5N and 32 ± 4N for MD and CM, respectively. Both polypropylene directions statistically fell into group A, while MD UM39 and CM UM39 were grouped into B and C, respectively. The UM39 seam strength was therefore found to be statistically significantly greater than the polypropylene gown. As such, the UM39 heat sealing method was determined to produce a stronger seal between sheets of field material than the ultrasonic welding method used in the polypropylene gown.

It is noted however from analysis of **Figures 3.3** and **3.5**, that the UM39 seamed samples demonstrated greater variability in tensile strength than the continuous samples. The variability

is likely due to the imprecision of heat application from the clothing iron used to heat seal the samples; it is anticipated that controlled industrial processes would address this inconsistency.

3.2 Contact Angle Testing

Contact angle testing was performed on UM39 samples of various fabrication and post-processing methods to determine if the different treatments had a significant impact on the hydrophobicity of UM39. Representative samples of similar coat weights (approximately 37gsm) were chosen from three treatments: drawdown coating (as per Section 2.2.1), hot press coating (as per Section 2.3.1), and hot press coating with embossing (see Section 5.2). A sample of the AAMI Level 3 polypropylene gown was also examined and compared against the UM39 samples listed. The measured contact angles of the samples are shown below in **Figure 3.6**, which presents a plot of specimen vs contact angle.

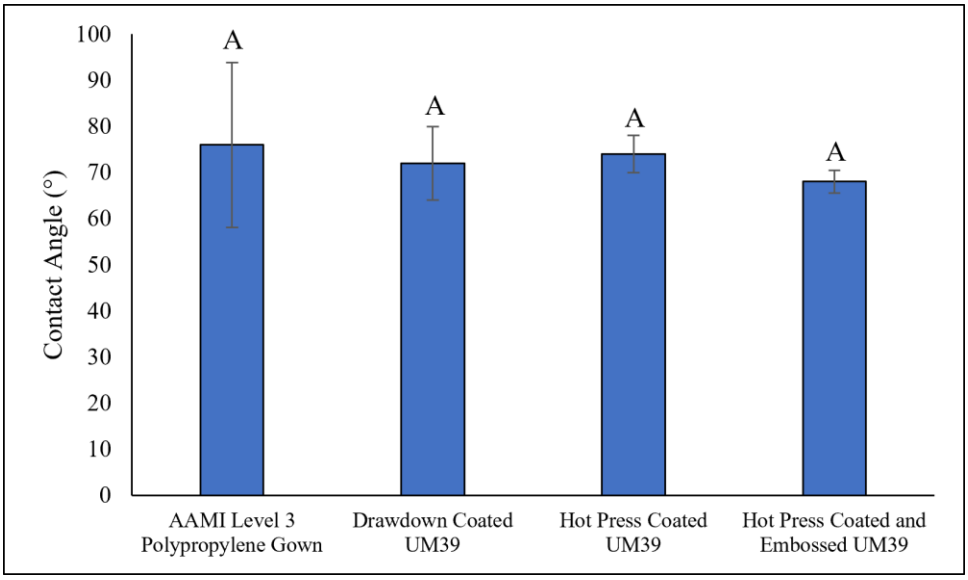

Figure 3.6. Contact Angle Testing Results from an on-market polypropylene isolation gown and UM39 fabricated from a variety of methods. Statistical differences are designated by differing letter annotations.

All samples demonstrated a similar contact angle of approximately 72 ± 9°, with all groups being statistically similar. As such, between the UM39 groups, the coating method (drawdown vs hand rolling and hot press curing) was not found to produce a significant change in the hydrophobicity of the material, nor was the addition of an embossing step. Furthermore, no significant difference in contact angle was found between any of the UM39 groups and the on-market polypropylene gown. Therefore, the contact angle of the UM39 material was found to be statistically equivalent to an on-market Level 3 isolation gown.

3.3 Full-sized Gown

3.3.1 Full-sized Gown Wearability

A full-sized isolation gown was fabricated via the method described in Section 2.3.2. An image of the gown prior to sleeve seaming is presented in **Figure 3.7**.

Figure 3.7. Image of isolation gown made from UM39 material.

The gown itself, while fully covering the exposed areas of the user, was found to be stiffer and more difficult to move in than conventional isolation gowns. The rigidity of the gown resulted in unintentional tearing of the gown when making movements that would stretch a more conventional material. While problematic, a number of investigative directions could potentially be taken to resolve this issue; results from one such exploratory investigation, namely embossing, are described in Section 5.2.

3.3.2 Full-sized Gown Barrier Performance

Samples of the two 3ft x 6ft sheets that were used to create the prototype gown were tested for their barrier properties to affirm that the assembled gown met PB70 Level 3 classification. Specifically, the barrier properties of the hand rolled and hot press cured UM39 material and previously described drawdown coated UM39 materials were evaluated with the

impact penetration and hydrostatic pressure tests. **Figure 3.8** presents plots of (a) specimen vs water penetration and (b) specimen vs hydrostatic failure pressure.

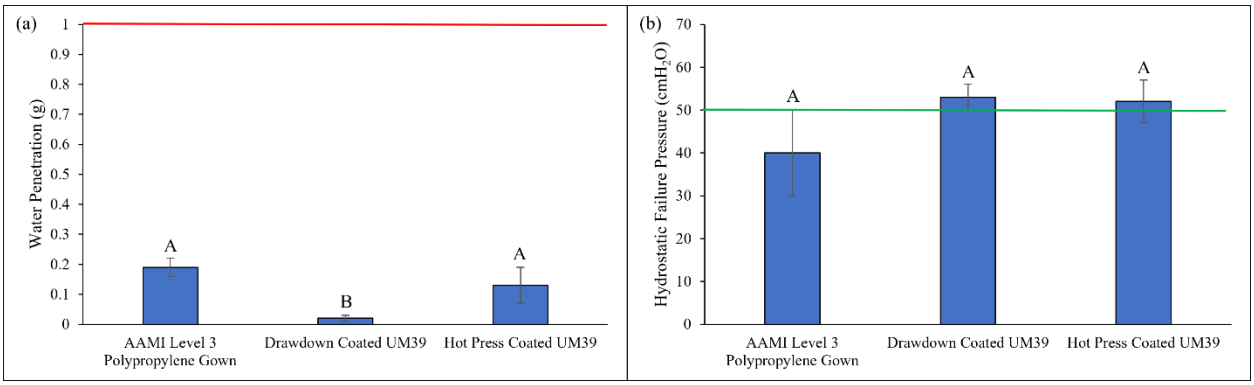

Figure 3.8. (a) AATCC 42 Impact Penetration Testing Results of the polypropylene gown, drawdown coated UM39, and hot press cured UM39 materials with the maximum allowed water penetration for Level 3 classification denoted by the red line. (b) AATCC 127 Hydrostatic Pressure Testing Results of the polypropylene gown, drawdown coated UM39, and hot press cured UM39 materials with the minimum allowable failure pressure for Level 3 classification denoted by the green line. Statistical differences are designated by differing letter annotations.

Investigation of **Figure 3.8a** reveals that the on-market polypropylene gown suffered the greatest water penetration, followed sequentially by the hot press coated UM39, and the drawdown coated UM39. The polypropylene gown and hot press coated UM39 were found to be statistically similar and both statistically different to the drawdown coated UM39. Further it is noted that the standard deviation of the hot press cured UM39 was greater than either the standard deviations of the polypropylene gown or the drawdown coated UM39; a fact that likely attests to the far greater variability in the hand rolled coating method employed in the scaled-up coating/curing process relative to the drawdown method. However, it is noted that although the hand rolled and hot press cured UM39 was more easily penetrated by water compared to the drawdown coated UM39 material, the hot press cured UM39 resisted more water than the on-market polypropylene material and far exceeded the less than 1g of water penetration requirement of the F3352 standard for PB70 Level 3 classification.

Examination of **Figure 3.8b** demonstrates that the drawdown coated UM39 displayed the greatest degree of hydrostatic barrier resistance, followed sequentially by the hand rolled and hot press cured UM39 and the polypropylene gown. Although all three groups were found to be statistically equivalent, only the drawdown coated and hot press cured UM39 materials passed the 50cmH_2O requirement to be classified as a PB70 Level 3 material. However, as seen in the impact penetration resistance testing, the standard deviation of the hot press cured UM39 material was greater than that of the drawdown coated material. The difference in standard deviation further exemplifies the greater variability of the hand rolled coating inherent to the hot press process compared to the rod coating of the drawdown process. Fortunately, as drawdown coating more accurately reflects conventional industrial-scale paper coating processes than hand rolled coating, it is hypothesized that future work in pilot-scale coating trials will likely also demonstrate lower standard deviations in barrier properties. It should be noted however that although the hot press coated material demonstrated greater variability in barrier properties than the drawdown coated material, a full-sized, fully compliant PB70 Level 3 isolation gown was nonetheless fabricated from the UM39 textile.

3.3.3 Full-sized Gown Paper and Coating Quantities

In addition to laboratory testing, a study to determine the required paper and coating quantities to create a full-sized gown was performed. Unfortunately, due to non-disclosure agreements between the University of Maine and the suppliers of the paper and coating materials, a monetary value could not be associated with the supply of paper or coating. However, the quantity of paper and coating required to create each gown was determined. From the SOLIDWORKS model described in Section 2.3.2, it was calculated that each gown consists of 2.055m^2 of paper substrate. However, as a gown must be excised from a larger sheet of coated

paper, a sheet of the maximum length and width of the two-dimensional template would more accurately reflect the total amount of paper necessary to create a gown. As such, the distances between the two arm cuffs of the gown and the top and bottom of the gown were used to determine that a sheet of 138.5cm x 191cm was required to fabricate a single gown. Therefore, 2.645m^2 of paper substrate is required to fabricate a single gown.

In addition to the paper substrate, the volume of coating required per gown was calculated. As in the paper substrate calculations, two volumes were determined: the first for the amount of coating per gown and the second for the amount of coating required per sheet from which a gown would be excised. Assuming a coat weight of 36gsm, approximately 71.83mL of coating would be used per gown, and 92.45mL of coating would be required to create a 138.5cm x 191cm sheet of UM39.

CHAPTER FOUR: Composting Trial Results

4.1 Initial Ranging Study

Although both components (the base sheet and the coating) of the UM39 material were likely compostable, a ranging study was performed to determine the extent and rate of degradation. Twelve 11cm x 11cm sheets of UM39 of 31 ± 1gsm coat weight and twelve 11cm x 11cm sheets of paper substrate control samples were inserted into a windrow. Triplicates of each sample type were removed and evaluated after 3, 7, 24, and 52 days via the method described in Section 2.6.1. In addition to the sheet samples, three 2cm x 21cm strip samples of UM39 were inserted into the windrow for a period of 21 days to investigate the role, if any, of sample geometry in the degradation process. Images of the samples post-removal from the windrow are presented in **Figure 4.1**.

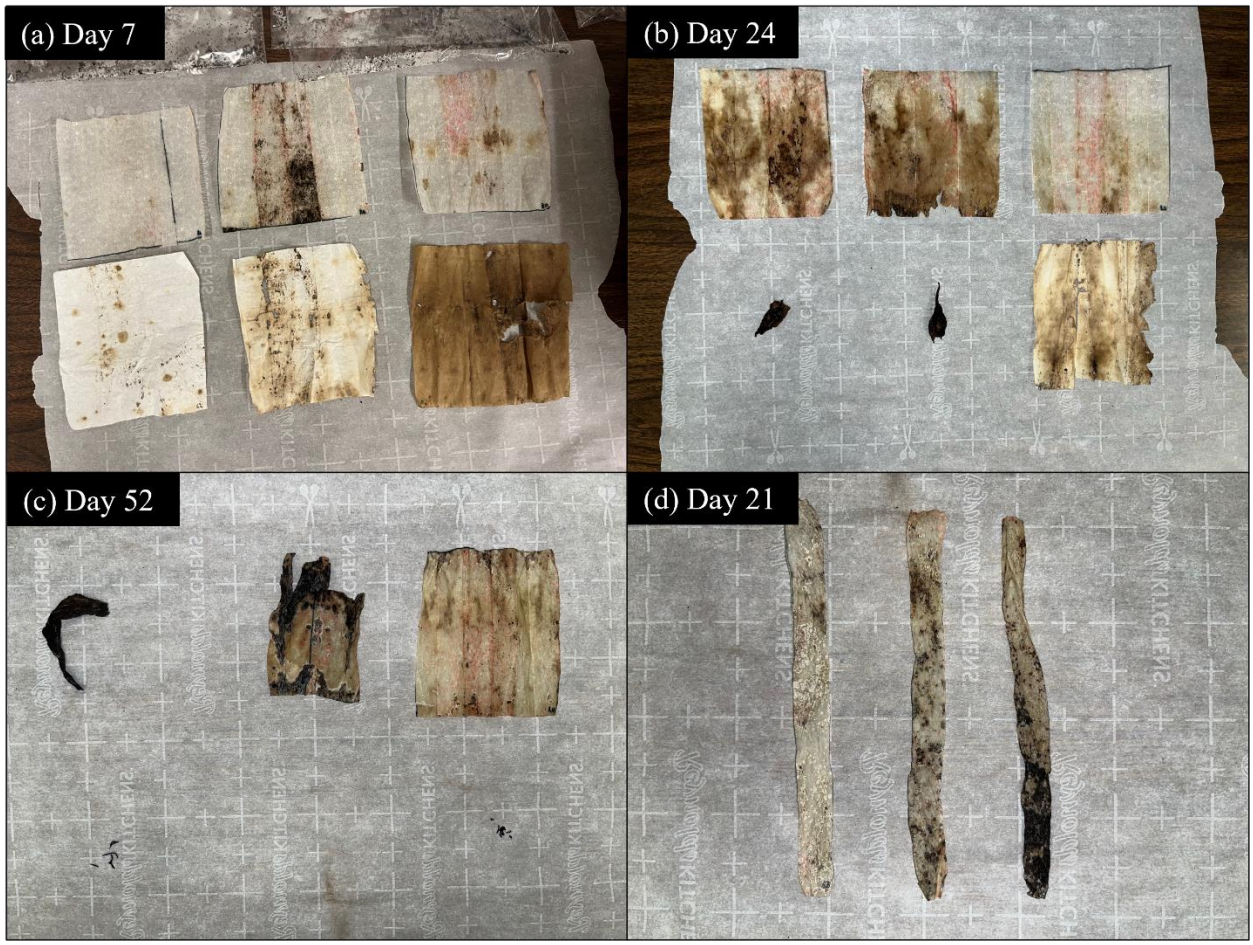

Figure 4.1. Appearances of composted UM39 (top row of each image) and paper substrate (bottom row of each image) samples removed from the windrow prior to oven drying. (a) 11cm x 11cm samples removed after 7 days in the windrow. (b) 11cm x 11cm samples removed after 24 days in the windrow. (c) 11cm x 11cm samples removed after 52 days in the windrow. (d) 2cm x 21cm samples removed after 21 days in the windrow.

Qualitative examination of the uncoated control samples in **Figure 4.1** demonstrates a trend of progressive decomposition over a period of 52 days under industrial composting conditions. Of the control samples removed after 7 days, discoloration was seen in two of the three samples with minor holes having been formed in the most discolored sample. After 24 days, two of the control samples had shrunk significantly and turned completely black, while the third sample demonstrated signs of discoloration and fringed edges, potentially indicating microbial decomposition of the sides of the sheet. Finally, after 52 days, one control sample had completely disintegrated, and the remaining control samples were completely black and

composed of disconnected fragments which were millimeters in length. As such, the uncoated paper substrate controls appeared to have nearly fully degraded after a period of 52 days under industrial composting conditions.

The UM39 samples were also found to demonstrate a progressive decomposition trend with time, however, not as rapidly, nor to the same extent as the uncoated paper controls. After 7 days, some discoloration was seen in two of the UM39 samples with the third sample displaying a rectangular area of discoloration, likely coinciding with the surface interfacing with the surrounding compost. UM39 samples removed after 24 days displayed more discoloration than the samples removed after 7 days. Furthermore, one of the 24-day UM39 samples displayed a fringed edge, potentially indicating microbial breakdown. Two of the UM39 samples removed after 52 days demonstrated progressively greater degradation due to the compost environment including extreme discoloration and shrinking, although with a significant degree of variation between samples. However, the last 52-day sample solely displayed discoloration. As such, the UM39 sheet samples were found to progressively decompose, although more slowly than the uncoated paper control samples.

The last sample group, the UM39 2cm x 21cm strip samples, were subject to industrial composting conditions for a shorter duration of time, namely 21 days. After composting, the strip samples demonstrated more discoloration than the analogous Day 24 coated sheet samples and displayed blemishes, such as the appearance of white and brown dots throughout the strips. The geometry of the samples, however, did not appear to be significantly altered. As such, although the strip samples demonstrated more discoloration compared to the analogous sheet samples, limited microbial breakdown was observed.

Based on the qualitative appearances of the paper substrate control and UM39 samples, the uncoated samples demonstrated the greatest degree of degradation. The UM39 samples were found to degrade to some extent after a period of 52 days in the windrow, however with a significant degree of variation. Furthermore, the UM39 strip samples were shown to demonstrate greater discoloration than the sheet samples which resided in the windrow for a similar period of time. In order to quantify the extent of sample degradation, the dry mass of each sheet was determined at the relevant time point per the experimental protocol outlined in Section 2.6.1. **Figure 4.2** presents a plot of time in the windrow vs the average percentage mass change of sample groups withdrawn at given time points. Note that the confidence limits indicate the standard deviation of the percent mass change of the relevant group.

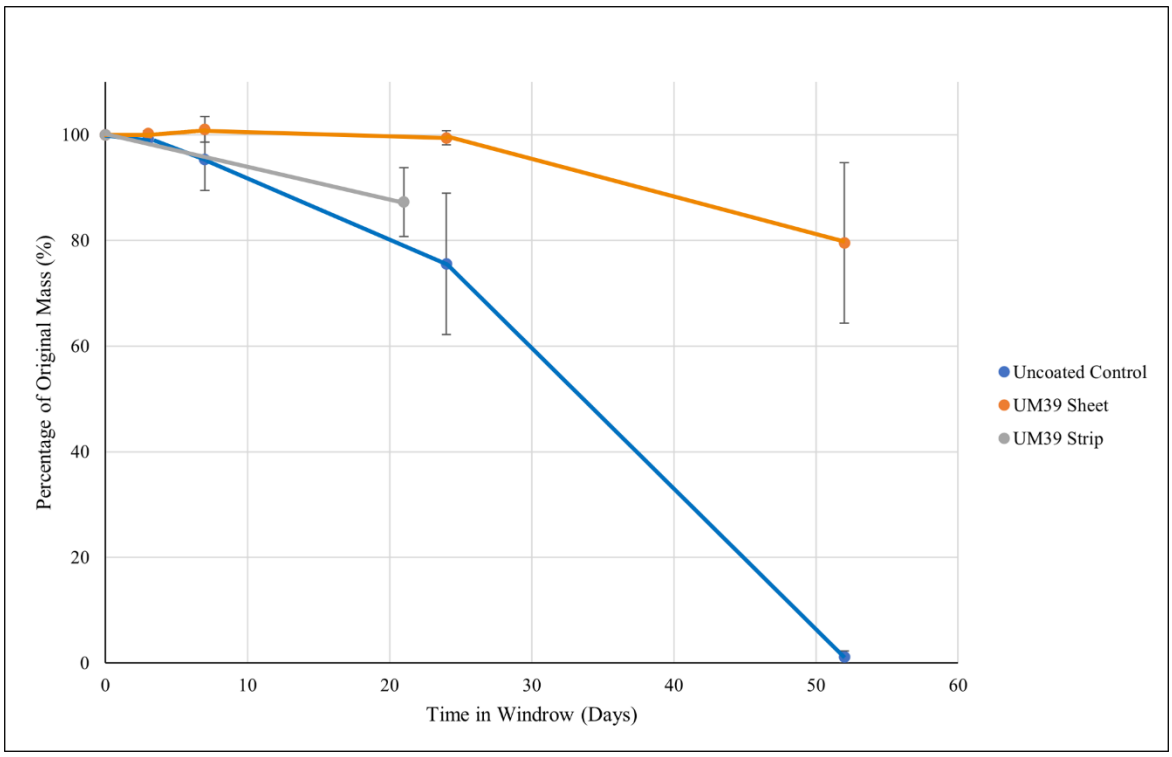

Figure 4.2. Degradation of UM39 sheet, UM39 strip, and uncoated paper substrate samples represented by the percentage of original mass as a function of time. The percentage of remaining mass was determined by the proportion of each sample's final dry weight to its initial dry weight. The percentage of remaining mass for 11cm x 11cm uncoated control, 11cm x 11cm UM39, and 2cm x 21cm UM39 samples are denoted by the blue, orange, and gray lines respectively.

Analysis of the data in **Figure 4.2** demonstrates an overall trend consistent with the qualitative observations. Specifically, the greatest and most rapid degradation occurred for the uncoated control samples, followed sequentially by the UM39 strip samples, and lastly the UM39 sheet samples. The remaining percentage of the original mass of the uncoated paper substrate control samples, represented by the blue line, exponentially decreased to 1 ± 1% over a period of 52 days. The mass of the UM39 sheet samples represented by the orange line, however, remained near 100% for 24 days and subsequently decreased to 80 ± 20% after a period of 52 days. Finally, the mass of the UM39 strip samples, represented by the gray line, after just 21 days under industrial composting conditions decreased to a remaining mass percentage of 87 ±

7%. As such, the overall trends of the samples' degradation indicate that the UM39 material displays a slower rate of degradation than the uncoated paper samples. However, it is important to note that significant degradation (~20%) of the UM39 sheets did occur at the 52-day mark, indicating that the coated material does in fact compost, although not as quickly as the uncoated substrate material. Furthermore, since the strip samples degraded to a similar extent as the sheet samples but in approximately half of the time, it appears likely that sample geometry plays a significant role in the rate of degradation. In order to assess the extent of the apparent effect of sample geometry on the rate of degradation, a statistical analysis was performed. **Figure 4.3** presents the average percentage mass change of sample groups withdrawn at their final time point. Note that the confidence limits indicate the standard deviation of the mass change of the relevant group.

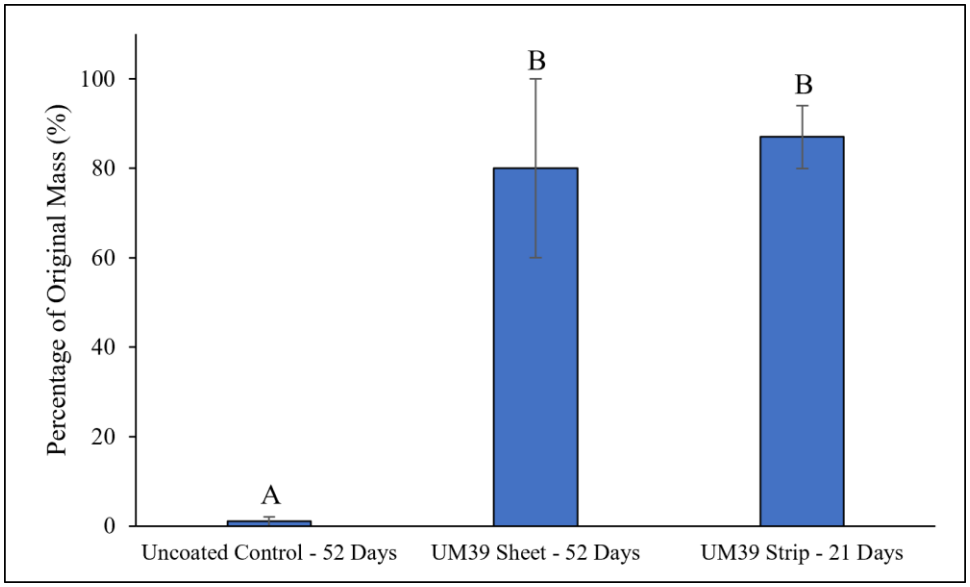

Figure 4.3. Average degradation of uncoated substrate, UM39 sheet, and UM39 strip samples withdrawn at their final timepoint. Statistical differences are designated by differing letter annotations ($P < 0.05$).

Analysis of **Figure 4.3** indicates a statistical difference between the uncoated control and UM39 sample groups and statistical similarity between the sheet and strip UM39 groups. As such, the change in sample geometry of the UM39 strip samples produced a statistically similar result to the UM39 sheet samples that were under industrial composting conditions for an additional three weeks. As such, an apparent relationship between degradation time and geometry was revealed. It is believed likely that the acceleration of degradation found in the strip samples is likely due to the greater environment-accessible surface area. As presented in **Figure 4.4**, the sheet samples were found to regularly fold in on themselves due to the constrictive nature of the Nylon mesh bags that the samples were placed in for visibility and containment inside the windrow. The strip samples, however, typically remained unfolded and thus their full surface area was in contact with the environment of the windrow and its entrained microbes. It is hypothesized therefore that the strip samples were able to interact with the surrounding microbes more than the sheet samples.

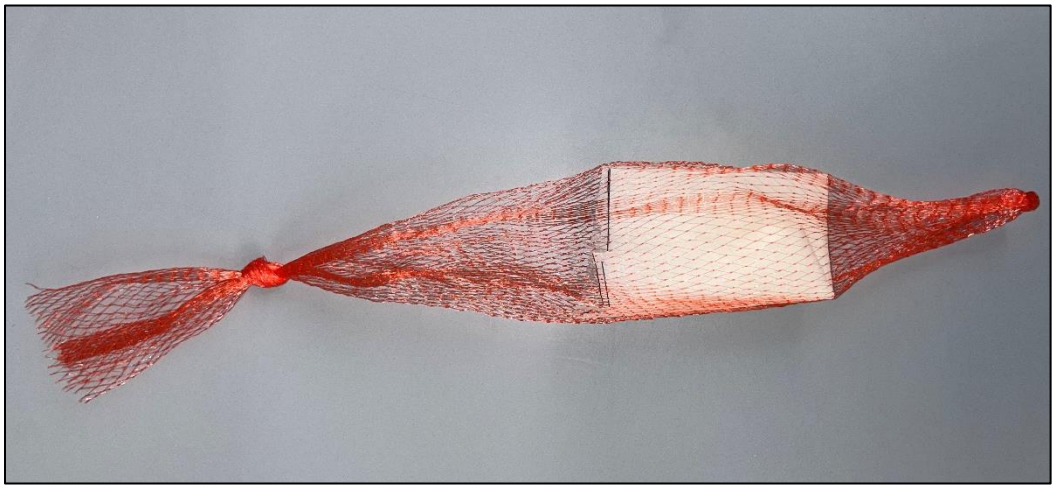

Figure 4.4. Nylon bag containing a folded 11cm x 11cm uncoated control sample. Note that the sample is constricted by the bag and folds in on itself.

Although quantitative signs of degradation were seen in the UM39 samples, the uncoated paper substrate controls degraded to a much greater extent to 1 ± 1% of their original mass. It is

hypothesized that the difference in degradation time between the paper substrate and UM39 samples is due to the presence of a hydrophobic coating on the UM39 materials (note the high sessile drop contact angle measurement depicted in **Figure 2.10**). The coating likely provided a less amenable object for the microbes in the windrow to interact with compared to an uncoated paper control. However, as the UM39 samples did display quantitative measures of degradation, it is evident that the microbes are eventually able to break down the UM39 material. Therefore, the ranging trial demonstrated that the UM39 material was degradable in an industrial windrow, however an extended trial was necessary to determine the approximate timeframe for complete degradation.

4.2 Extended Duration Study

Upon completion of the ranging study, an extended duration study was designed which incorporated minor changes in the experimental procedure of the ranging study, which were influenced by the ASTM 6868 standard. The primary requirement of the standard for a material to be classified as industrially compostable is that the tested samples of the material must have less than 10% of their initial dry mass remaining after a period of 84 days (per the ISO 16929 test). While the ISO 16929 standard traditionally requires a benchtop laboratory test using a controlled environmental chamber, the practicality of testing the material in an established and in-use industrial composting facility was determined to be preferable to accurately evaluate the compostability of the UM39 material under practical composting conditions. As such, the incorporation of the ISO 16929 standard procedures primarily affected the testing protocol, sample size, and length, rather than the environment in which the samples resided.

In the extended study, UM39 of 30 ± 4gsm coat weight and paper substrate samples were tested as described in Section 2.6.2. Images of the samples post-removal from the windrow and sieving are presented in **Figure 4.5**.

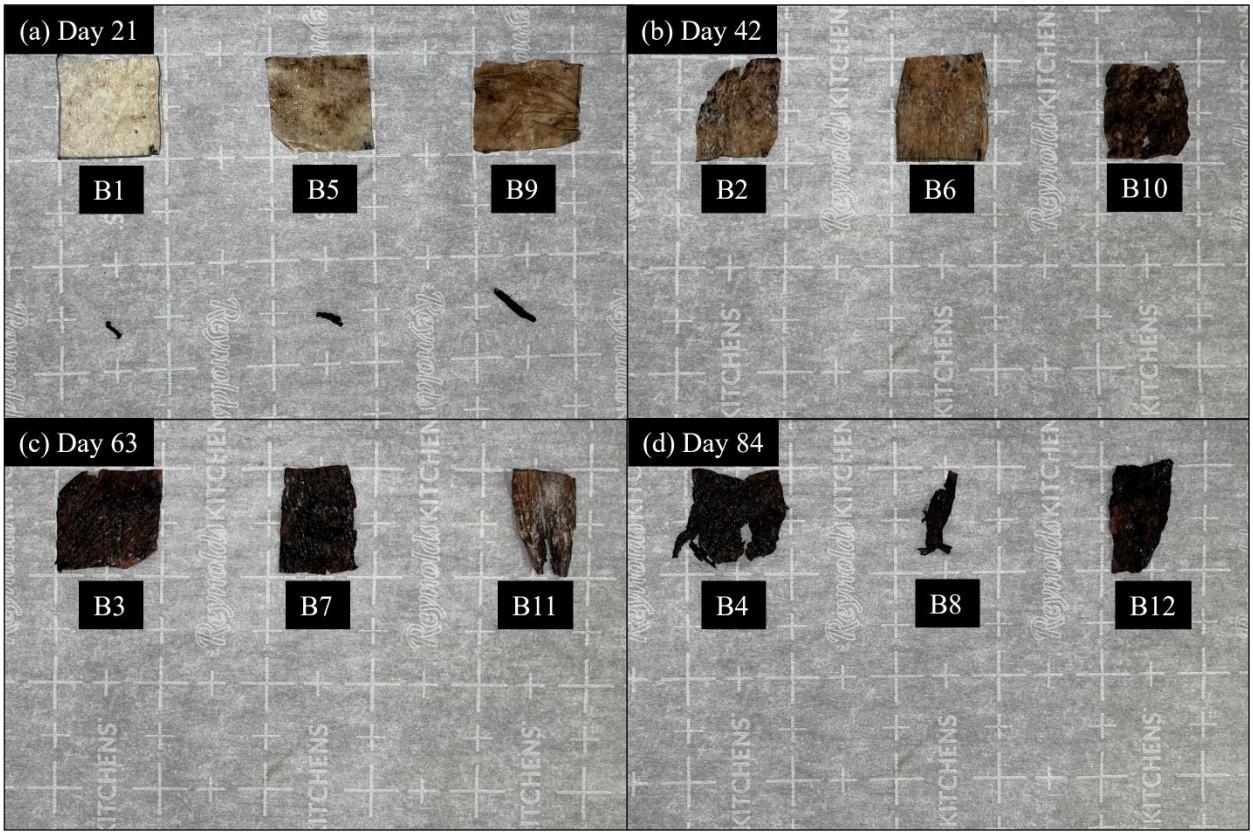

Figure 4.5. Appearances of composted UM39 (top row of each image) and paper substrate (bottom row of each image) samples removed from the windrow prior to drying. (a) 5cm x 5cm UM39 and paper substrate samples removed after 21 days in the windrow. (b) 5cm x 5cm samples removed after 42 days in the windrow. (c) 5cm x 5cm samples removed after 63 days in the windrow. (d) 5cm x 5cm samples removed after 84 days in the windrow.

Analysis of **Figure 4.5** demonstrates an overall trend of the uncoated control samples rapidly degrading before 42 days, and the UM39 samples progressively degrading over a period of 84 days. **Figure 4.5a** displays samples B1, B5, and B9 as well as three uncoated paper control samples at 21 days. The control samples had turned fully black and shrunk into thin, elongated rod-like fragments. The UM39 samples, however, remained largely the same shape with varying

degrees of discoloration. **Figure 4.5b** displays the UM39 samples B2, B6, and B10 at 42 days. The uncoated control samples were found to have fully degraded and thus are not pictured on day 42 or at any further timepoints. The three UM39 samples all demonstrated different qualities after degradation. Sample B2 was dry, discolored, and appeared to have shrunk, sample B6 was dry, and discolored, but did not appear to have changed in size, and sample B10 was moist and demonstrated signs of degradation such as significant darkening and fringing of the edges. **Figure 4.5c** displays samples B3, B7, and B11 at 63 days. Samples B3 and B7 had turned nearly completely black, while sample B11 maintained a much lighter shade, appearing similar in color to sample B5 which had only resided in the windrow for 21 days. Furthermore, samples B3 and B7 were similar in wetness to sample B10, potentially indicating a degradation of the coating, which allowed moisture ingress. Sample B11, however, demonstrated the greatest decrease in size and was dry. Lastly, **Figure 4.5d** displays samples B4, B8, and B12 at 84 days. Samples B4 and B12 were observed to be wet upon removal from the windrow, while sample B8, which appeared to be the most degraded sample in the entire study, was dry. All three samples appeared nearly fully black indicating extreme discoloration, although sample B4 exhibited an apparent brittleness potentially correlated with the faint white dots speckled on the sample surface.

While the overall trend of the images in **Figure 4.5** seems to indicate a slow progressive degradation of UM39 under industrial composting conditions, the degradation route is unclear. The emergence of a wet sample after 42 days was remarkable as it indicated that the hydrophobic coating of the UM39 sample may have broken down in the windrow, thereby allowing moisture ingress. However, as the other Day 42 samples remained dry, the coating did not appear to degrade at the same rate for all samples. It should be noted that variation in local moisture content in the windrows was not a variable that could be controlled and may have led to sample

variation. Furthermore, of the last six UM39 samples collected on days 63 and 84, four were found to be wet, although the sample which appeared to have degraded to the greatest extent, B8, was found to be dry. As such, the qualitative observations of the composting study samples are not sufficient to draw conclusions with regard to the cause of the variation in degradation between the UM39 samples.

The qualitative observations of the samples upon removal from the windrow may be able to be contextualized by the change in their quantitative mass measurements. **Table 4.1** presents each sample's number of days in the windrow, initial ambient weight before composting, initial dry weight, degraded ambient weight following removal from the windrow and sieving, and degraded dry weight.

Table 4.1. Initial and final ambient and dry weights of composted UM39 samples.

Days in Windrow	Sample	Initial Ambient Weight (g)	Initial Dry Weight (g)	Degraded Ambient Weight (g)	Degraded Dry Weight (g)
21	B1	0.1764	0.1694	0.1942	0.1701
	B5	0.1680	0.1613	0.2037	0.1600
	B9	0.1700	0.1638	0.2010	0.1645
42	B2	0.1672	0.1690	0.1680	0.1284
	B6	0.1861	0.1791	0.2044	0.1652
	B10	0.1711	0.1645	0.2962	0.1102
63	B3	0.1796	0.1731	0.3803	0.1415
	B7	0.1893	0.1828	0.4588	0.1640
	B11	0.1731	0.1662	0.1687	0.1390
84	B4	0.1950	0.1879	1.1247	0.3518
	B8	0.1690	0.1627	0.1296	0.0670
	B12	0.1913	0.1834	0.3782	0.1720

Analysis of **Table 4.1** demonstrates that the five UM39 samples that were observed to be wet, B3, B4, B7, B10, and B12, all shared a characteristic significant increase in degraded ambient weight from initial ambient weight. It is hypothesized that this increase in ambient

weight is the result of liquids in the windrow penetrating into the UM39 samples. While most other samples demonstrated an approximately 1.1 times increase in degraded ambient weight compared to their initial ambient weight, the degraded ambient weight of the noticeably wet samples demonstrated a 1.8 to 6 times increase from their initial ambient weight. As such, it is hypothesized that the increase in weight is attributable to the uptake of liquids from the windrow into the paper substrate of the UM39 samples once the hydrophobic coating began to break down. The hypothesis is further justified by the change in degraded ambient weight to degraded dry weight of the samples. The five wet samples demonstrated a more drastic decrease in degraded ambient to degraded dry weight than the seven dry samples. For example, at 63 days, the change in mass from degraded ambient to degraded dry weight for the two wet samples B3 and B7 was -0.2388g and -0.2948g, respectively, while the change in mass of the dry B11 sample was only -0.0297g. The almost tenfold increase in the change in mass found in the wet samples compared to the dry sample after being oven dried at 105°C suggests that more water had been evaporated off the wet samples than the dry sample. Therefore, water must have had been absorbed by the wet samples in the windrow, which would likely not have been possible if the hydrophobic coating had not degraded at least to some extent. However, the absorption of surrounding materials in the windrow into the paper substrate may not have been exclusively water-based. Sample B4 presents an abnormality that may suggest that non-aqueous liquids were absorbed into the samples. The degraded dry weight of sample B4 is approximately twice its initial dry weight. As such, more mass was present on or in the UM39 sample after the composting process than before. It is hypothesized that once the hydrophobic coating degraded in the windrow, surrounding oil-based and aqueous substances were absorbed by the sample. Therefore, while the drying method was able to evaporate the water from the sample, the oils

remained, inflating the measured dry weight of the UM39 sample. The inflating effect is most obvious in sample B4; however, the effect may have occurred in the other samples once the hydrophobic coating began to break down in the windrow.

With the variations between tested UM39 samples in context, the measured average degradation of the samples can be analyzed. **Figure 4.6** presents a plot of time in the windrow vs the average percentage mass change of sample groups withdrawn at given time points. Note that the confidence limits indicate the standard deviation of the percent mass change of the sample group.

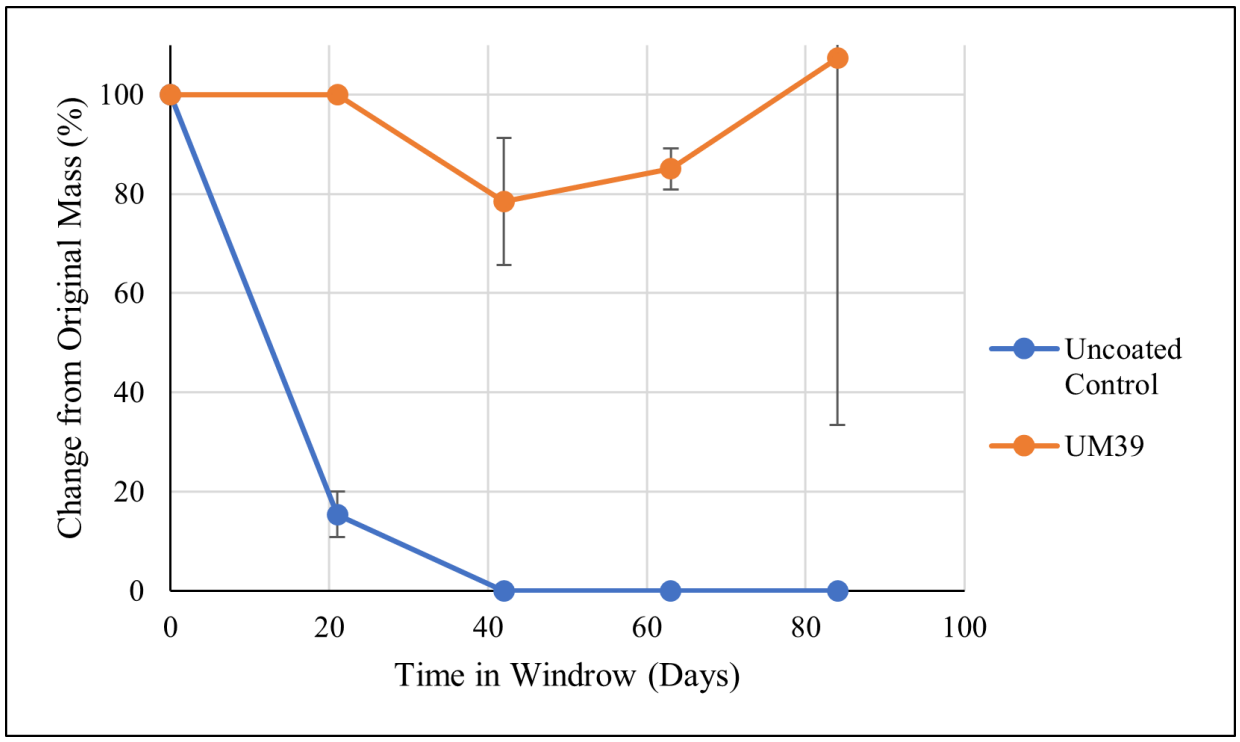

Figure 4.6. Degradation of 5cm x 5cm UM39 and uncoated paper substrate samples as a function of time for 84 days under industrial composting conditions. The percentage of remaining mass for the 5cm x 5cm uncoated control and 5cm x 5cm UM39 samples are denoted by the blue and orange lines, respectively.

Analysis of **Figure 4.6** indicates an overall trend of the uncoated paper control samples fully degrading within 42 days, consistent with the approximate timespan identified in the ranging study (see **Figure 4.2**). The UM39 samples, however, demonstrated an unexpected trend. Instead of continuing to degrade over time, the samples appeared to have decreased in mass for the initial 42-day period and subsequently increased in mass until day 84. Furthermore, the samples measured at 84 days exhibited an extremely large standard deviation. Specifically, the UM39 samples remained at a near constant mass for 21 days, decreased to 80 ± 10% after 42 days, then rose to 85 ± 4% after 63 days, and further increased to 110 ± 70% after 84 days. Closer investigation of the 84-day samples revealed that samples B4, B8, and B12 were measured to be 187%, 41%, and 93% of their original dry weight, respectively. A multitude of factors could contribute to this extreme variation. Firstly, the B4 and B12 samples were both wet upon removal from the windrow. The moisture of the samples would indicate that the hydrophobic coating had at least partially degraded during composting, therefore one may assume that these wet samples would display quantitative signs of degradation. However, the remaining percentage of dry mass of these wet samples was much greater than that of the dry sample B8. Two hypotheses are proposed for the cause of this unexpected result. The first hypothesis, as previously described, is that after a period of 42 days, the hydrophobic coating of the UM39 material begins to break down, as evidenced by the emergence of a wet UM39 sample at 42 days. Afterwards, the substrate would become permeable to both water and oil-based liquids. The water-based liquids would be able to evaporate from the substrate in the oven drying process, however the oils would not. As such, the apparent dry mass of the remaining UM39 sample would become inflated.

However, an alternative degradation route exists if the hydrophobic coating did not degrade before the rest of the UM39 material and instead portions of the coating and substrate of the UM39 sample degraded simultaneously. The measured mass of the remaining UM39 sample would therefore decrease while remaining dry. As such, samples B4 and B8 may resemble two different degradation routes: wet and dry. In wet degradation, the breakdown of the coating may allow oils to be absorbed into the UM39 samples and prevent degradation. Whereas in dry degradation, the hydrophobic coating and paper substrate may degrade simultaneously, not allowing for the absorption of oils from the surrounding windrow environment. The measurement of oil content and homogeneity in distribution throughout the windrow would require further investigation in future studies to confirm this hypothesis.

An alternative hypothesis for the cessation of degradation of the UM39 samples at approximately 42 days is a lack of microbial activity in the windrow. **Figure 4.7** displays a plot of the windrow temperature at each sample location on the left abscissa and average percentage mass change of sample groups on the right abscissa, as a function of time in the windrow on the ordinate.

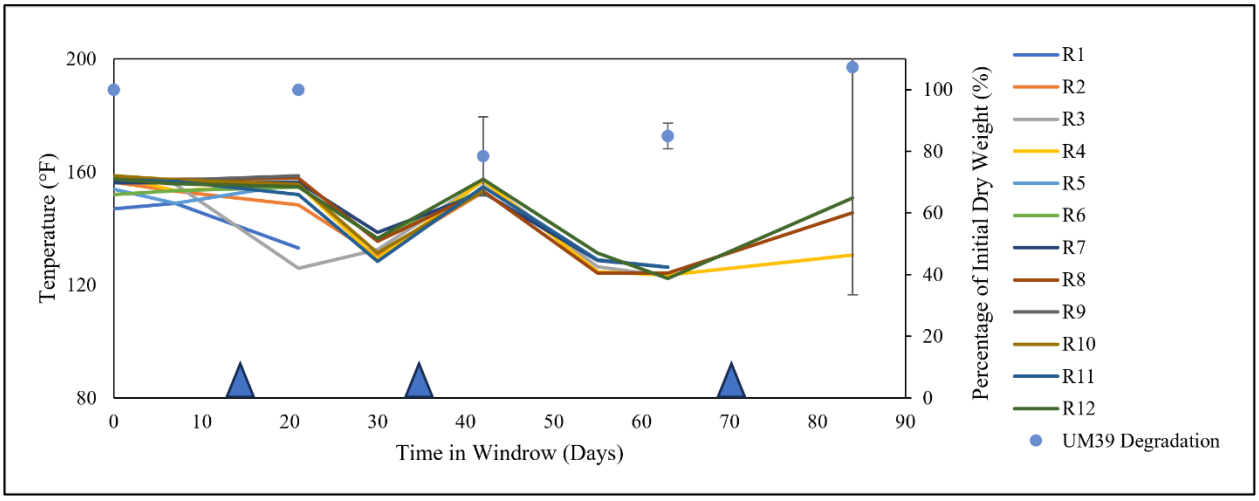

Figure 4.7. Plot of windrow temperature (left abscissa) at each sample location and percentage of initial dry mass of the UM39 samples (right abscissa) as a function of time over a period of 84 days (ordinate). Blue triangles on the ordinate mark the days on which on the windrow was turned.

Analysis of **Figure 4.7** indicates that the temperature of the windrow at each sample location was approximately 160°F at the beginning of the study. The overall trend of the temperature demonstrates an initial high constant temperature for approximately 20 days, followed by a near 20°F decrease over a 10-day period, a sharp increase back to 160°F over a 14-day period, and a more gradual decline to 120°F over a 30-day period. The upward trends in the temperature profiles are correlated with windrow turning, which occurred on days 14, 35, and 70, as indicated by blue triangles on the ordinate of **Figure 4.7**. The need for the turning of the windrow was determined by the CompostManager software used at Casella Organics Hawk Ridge based on the readings of the CompostManager probe (see Section 2.6.1). It is important to note that windrows are typically deconstructed and shipped as compost after a period of approximately 40 days. As such, the conditions of windrows post-40 days are not typically known or experienced. It should be noted that it is possible that the CompostManager software did not flag the windrow used for the degradation study as needing to be turned as frequently

after a period of 40 days, as the windrow was determined to be ready for deconstruction and shipment. The decrease in temperature after 40 days infers that the microbial activity post-40 days in the windrow would be significantly reduced relative to when the windrow was first constructed. The lack of microbial activity is evidenced by the nearly month-long 120°F region in the temperature profile. A further study placing the samples into a new windrow after a period of 40 days would be required to determine if the lack of sample degradation after 40 days is a direct result of a loss of microbial activity.

Although inconclusive with regard to the industrial compostability of UM39, the extended composting study illuminated many aspects of the material. Two degradation routes were observed with samples removed from the windrow after 40 days: namely wet or dry degradation. Furthermore, the sample that experienced the greatest quantitative degree of degradation after a period of 84 days was found to be dry after removal from windrow and had degraded to 41% of its initial dry mass. However, the reduction in temperature and thus microbial activity in the windrow may have negatively affected the degradation of the UM39 samples. Regardless, the extended composting study demonstrated that UM39 displays both qualitative and quantitative signs of degradation when inserted into an industrial windrow composting process.

CHAPTER FIVE: Conclusions and Future Directions

5.1 Conclusions

The ever-increasing amount of synthetic polymer-based waste generated each year presents a major ecological and global health challenge. Healthcare systems in particular are a significant contributor to this issue due to the amount of single-use synthetic polymer-based personal protective equipment used for both healthcare workers and patients. As the majority of personal protective equipment waste by weight is comprised of isolation gowns, a need exists for alternatives to the traditional synthetic polymer-based gowns used by healthcare workers and patients. To best meet this need, a compostable isolation gown textile was engineered.

A multitude of paper substrates and coating formulations were evaluated as candidates to create a lightweight coated paper isolation gown textile. Paper substrates of tissue and towel materials were selected based on their softness, drape, and strength. The substrates were coated with an industrially compostable aqueous formulation of VerdeCoat™ to grant the barrier properties necessary for user protection. The five tests required to classify a material as a textile suitable for use as a Class 3 isolation gown, the AATCC 42, AATCC 127, D5034, D5733, and D1683 tests, were subsequently conducted on coated paper substrates (of 29gsm and 39gsm basis weight and coat weights of approximately 16gsm and 36gsm, respectively) and commercial polypropylene textiles. The UM39 textile, comprised of a 39 gsm basis weight hand towel and an approximately 36 gsm coating of VerdeCoat™, was demonstrated to exceed all of the requirements necessary for PB70 Level 3 classification and in some cases performed better than an on-market polypropylene gown.

From the UM39 textile, a full-sized isolation gown was fabricated. Although the prototype was found to be stiffer than current synthetic polymer isolation gowns, the design

demonstrated great potential as a lightweight, high-protection gown assuming that future work can increase its drape. In addition, a composting study was conducted to evaluate the degradability of the UM39 material under industrial composting conditions. The UM39 material was found to exhibit qualitative and quantitative signs of degradation beginning after a period of 42 days in a windrow. Given the fact that the material surpassed all required standardized tests for use as a Class 3 isolation gown and was shown to degrade under industrial composting conditions, the developed UM39 textile was demonstrated to be a promising alternative to traditional synthetic polymer isolation gowns.

5.2 Future Directions

To move the UM39 gown prototype towards commercialization, future work should be conducted to quantify its performance in pilot-scale coating trials as well as its viability for converting. In addition, its industrial compostability should be further investigated. As such, a study investigating the effect of incorporating the active composting stage of the industrial process could be beneficial to determining the degradability of UM39 in a practical environment. As stated in Section 4.2, such a study would be challenging and could pose safety risks. As such, a viable alternative would be another extended duration study in which the samples were relocated into a fresh windrow after a period of 40 days to maintain a higher level of microbial activity. In addition, an analysis of the composted material may provide further insight into the degradability of UM39. As such, a study examining the composted materials' chemical and microbial composition should be conducted to determine the mechanism by which the UM39 samples are degraded under industrial composting conditions.

A concern with the current UM39 prototype gown is its stiffness and therefore wearability. A potential approach to decrease the material's stiffness and increase its drape is to

emboss it. Embossing is a technique used to create textured patterns on the surface of a material by applying pressure and heat to deform the material's internal structure. A preliminary embossing trial has demonstrated a potentially promising pathway to decrease the stiffness of the material. A low-heat, shallow-texture New Seville pattern was embossed through a 381 Embosser on to 6in x 18in samples of UM39 at SAPPI North America in its Westbrook facility. The embossed samples were found to have decreased stiffness, better drape, and a softer texture than similar non-embossed samples. As such, a future comprehensive embossing trial should be conducted on UM39 samples to optimize the wearability and comfort of the gown.

An alternative approach to addressing the stiffness of the UM39 gown would be to investigate the viability of other on-market barrier coatings aside from VerdeCoat™. Whereas in the presented work, the effect of coat weight on barrier performance was primarily investigated, the use of other types of industrially compostable functional coatings may provide sufficient barrier properties with reduced stiffness. Once the stiffness of the gowns is addressed, additional full-sized compostable isolation gowns should be created and used for a wearability analysis to confirm the potential of UM39 for use as personal protective equipment in healthcare settings.

REFERENCES

1. Vongdala, N., Tran, H. D., Xuan, T. D., Teschke, R. & Khanh, T. D. Heavy metal accumulation in water, soil, and plants of municipal solid waste landfill in Vientiane, Laos. *Int J Environ Res Public Health* **16**, (2019).

2. National Overview: Facts and Figures on Materials, Wastes and Recycling. *United States Environmental Protection Agency* (2022).

3. Talalaj, I. A. Assessment of groundwater quality near the landfill site using the modified water quality index. *Environ Monit Assess* **186**, 3673–3683 (2014).

4. Siddiqua, A., Hahladakis, J. N. & Al-Attiya, W. A. K. A. An overview of the environmental pollution and health effects associated with waste landfilling and open dumping. *Environmental Science and Pollution Research* **29**, 58514–58536 (2022).

5. Blair, J. & Mataraarachchi, S. A review of landfills, waste and the nearly forgotten nexus with climate change. *Environments - MDPI* **8**, (2021).

6. Shen, F. W., Guo, H. C. & Xin, C. L. The environmental assessment of landfill based on stakeholder analysis. *Procedia Environ Sci* **13**, 1872–1881 (2012).

7. Koda, E., Kiersnowska, A., Kawalec, J. & Osiński, P. Landfill slope stability improvement incorporating reinforcements in reclamation process applying observational method. *Applied Sciences (Switzerland)* **10**, (2020).

8. Dajić, A. *et al.* Landfill design: Need for improvement of water and soil protection requirements in EU Landfill Directive. *Clean Technol Environ Policy* **18**, 753–764 (2016).

9. Wijekoon, P. *et al.* Progress and prospects in mitigation of landfill leachate pollution: Risk, pollution potential, treatment and challenges. *J Hazard Mater* **421**, (2022).

10. Mataloni, F. *et al.* Morbidity and mortality of people who live close to municipal waste landfills: A multisite cohort study. *Int J Epidemiol* **45**, 806–815 (2016).

11. Textiles: Material-Specific Data | US EPA. https://www.epa.gov/facts-and-figures-about-materials-waste-and-recycling/textiles-material-specific-data.

12. Cho, H. W., Koo, H. J., Kim, H. & Kim, K. J. Lifetime Prediction of High Tenacity Polyester Yarns for Hydrolytic Degradation Used for Soil Reinforcement. *Fibers and Polymers* **21**, 1663–1668 (2020).

13. Uddin, M. A. *et al.* Environmental Impacts of Personal Protective Clothing Used to Combat COVID- 19. *Advanced Sustainable Systems* vol. 6 Preprint at https://doi.org/10.1002/adsu.202100176 (2022).

14. Rani, S. & Jamal, Z. *Recycling of Textiles Waste for Environmental Protection*. *~ 164 ~ International Journal of Home Science* vol. 4 www.homesciencejournal.com (2018).

15. Jain, N. & LaBeaud MD, D. How Should US Health Care Lead Global Change in Plastic Waste Disposal. *AMA J Ethics* (2022).

16. Jenkins, N. How to reduce waste by increasing use of reusable medical textiles. *Supply Chain Strategies & Solutions*.

17. Medical Gowns | FDA. https://www.fda.gov/medical-devices/personal-protective-equipment-infection-control/medical-gowns.

18. Mazahir, F. A. & Al Qamari, A. M. Personal protective equipment (PPE) and plastic pollution during COVID-19: strategies for a sustainable environment. *Rev Environ Health* **37**, 321–325 (2022).

19. Vozzola, E., Overcash, M. & Griffing, E. Environmental considerations in the selection of isolation gowns: A life cycle assessment of reusable and disposable alternatives. *Am J Infect Control* **46**, 881–886 (2018).

20. Das, K. P., Sharma, D., Saha, S. & Satapathy, B. K. From outbreak of COVID-19 to launching of vaccination drive: invigorating single-use plastics, mitigation strategies, and way forward. *Environmental Science and Pollution Research* (2021) doi:10.1007/s11356-021-16025-4/Published.

21. Saber, D. A., Howlett, B., Waterman, T. & de Tantillo, L. Solid waste and disposal processes for isolated patients with infectious disease. *Online J Issues Nurs* **23**, 1–1 (2018).

22. Considerations for Selecting Protective Clothing | NPPTL | NIOSH | CDC. https://www.cdc.gov/niosh/npptl/topics/protectiveclothing/default.html.

23. CDC. *Implementation of Personal Protective Equipment (PPE) Use in Nursing Homes to Prevent Spread of Multidrug-Resistant Organisms (MDROs)*. (2022).

24. Kilinc, F. S. A Review of Isolation Gowns in Healthcare: Fabric and Gown Properties. *J Eng Fiber Fabr* **180**, (2015).

25. Siegel, J. D., Rhinehart, E., Jackson, M. & Linda, ; *CDC Guideline for Isolation Precautions: Preventing Transmission of Infectious Agents in Healthcare Settings*. (2022).

26. van Dijk, M. D., Voor in ’t holt, A. F., Polinder, S., Severin, J. A. & Vos, M. C. The daily direct costs of isolating patients identified with highly resistant micro-organisms in a non-outbreak setting. *Journal of Hospital Infection* **109**, 88–95 (2021).

27. Johns Hopkins Center for Health Security. *Interim Estimate of US PPE Needs for COVID-19*. www.centerforhealthsecurity.org/PPE-assumptions. (2020).

28. Tsang, Y., Duffton, A., Leech, M., Rossi, M. & Scherer, P. Meeting the challenges imposed by COVID-19: Guidance document by the ESTRO Radiation TherapisT Committee (RTTC). in *Technical Innovations and Patient Support in Radiation Oncology* vol. 15 6–10 (Elsevier Ireland Ltd, 2020).

29. Verma, A., Patel, A. B., Tio, M. C. & Waikar, S. S. Caring for Dialysis Patients in a Time of COVID-19. *Kidney Medicine* vol. 2 787–792 Preprint at https://doi.org/10.1016/j.xkme.2020.07.006 (2020).

30. Collins, T. A. *et al.* Reuse of disposable isolation gowns in rodent facilities during a pandemic. *Journal of the American Association for Laboratory Animal Science* **60**, 431–441 (2021).

31. Kilinc Balci, F. S. Isolation gowns in health care settings: Laboratory studies, regulations and standards, and potential barriers of gown selection and use. *Am J Infect Control* **44**, 104–111 (2016).

32. Rutala, W. A. & Weber, D. J. A Review of Single-Use and Reusable Gowns and Drapes in Health Care. *Infect Control Hosp Epidemiol* **22**, 248–257 (2001).

33. McQuerry, M., Easter, E. & Cao, A. Disposable versus reusable medical gowns: A performance comparison. *Am J Infect Control* **49**, 563–570 (2021).

34. Lovitt, S. A., Nichols, R. L., Smith, J. W., Muzik, A. C. & Pearce, P. E. Isolation gowns: A false sense of security? *Am J Infect Control* (1992).

35. Medical Waste | US EPA. https://www.epa.gov/rcra/medical-waste.

36. Corbin, L. *et al.* A 24-hour waste audit of the neuro ICU during the COVID-19 pandemic and opportunities for diversion. *The Journal of Climate Change and Health* **8**, 100154 (2022).

37. F3352 Standard Specification for Isolation Gowns Intended for Use in Healthcare Facilities. *ASTM* (2019) doi:10.1520/F3352-19.

38. American Hospital Association. AHA Hospital Statistics, 2017 Edition. *https://www.aha.org/2016-12-27-aha-hospital-statistics-2017-edition* (2017).

39. Halpern, N. A. & Pastores, S. M. Critical care medicine beds, use, occupancy, and costs in the United States: A methodological review. *Critical Care Medicine* vol. 43 2452–2459 Preprint at https://doi.org/10.1097/CCM.0000000000001227 (2015).

40. Saber, D., Norris, A. E., Reinking, J., Trompeter, G. & Sanford, D. Analyzing the cost of hospital contact isolation practices: Implications for nursing administrator practice, research, and policy. *Journal of Nursing Administration* (2022) doi:10.1097/NNA.0000000000001160.

41. Kilinc-Balci, F. S., Nwoko, J. & Hillam, T. Evaluation of the Performance of Isolation Gowns. in *American Journal of Infection Control* vol. 43 S44 (Elsevier BV, 2015).

42. Granzow, J. W., Smith, J. W., Nichols, R. L., Waterman, R. S. & Muzik, A. C. Evaluation of the protective value of hospital gowns against blood strike-through and methicillin-resistant Staphylococcus aureus penetration. *Am J Infect Control* (1998).

43. ANSI/AAMI PB70. *CDC* http://www.cdc.gov/niosh/npptl/topics/protectiveclothing/#table3 (2021).

44. Kahveci, Z., Kilinc-Balci, F. S. & Yorio, P. L. Barrier resistance of double layer isolation gowns. *Am J Infect Control* **49**, 430–433 (2021).

45. Schirmer, A. *et al.* Isolation gowns as a potential work hazard. *Ann Work Expo Health* **64**, 596–603 (2020).

46. Municipal Solid Waste Landfills | US EPA. https://www.epa.gov/landfills/municipal-solid-waste-landfills.

47. Maturi, K. C., Haq, I., Kalamdhad, A. S. & Gupta, A. A glance over current status of waste management and landfills across the globe: A review. in *Biodegradation and Detoxification of Micropollutants in Industrial Wastewater* 131–144 (Elsevier, 2022). doi:10.1016/B978-0-323-88507-2.00001-4.

48. Salem, Z., Hamouri, K., Djemaa, R. & Allia, K. Evaluation of landfill leachate pollution and treatment. *Desalination* **220**, 108–114 (2008).

49. Deng, Y. Advanced Oxidation Processes (AOPs) for reduction of organic polluants in landfill leachate: a review. *Int J Environ Waste Manag* (2009).

50. Alkalay, D., Guerrero, L., Lema, J. M., Mendez, R. & Chamy, R. *Review: Anaerobic Treatment of Municipal Sanitary Landfill Leachates: The Problem of Refractory and Toxic Components*.

51. Bioreactor Landfills | US EPA. https://www.epa.gov/landfills/bioreactor-landfills.

52. Wojnowska-Baryła, I., Bernat, K. & Zaborowska, M. Plastic Waste Degradation in Landfill Conditions: The Problem with Microplastics, and Their Direct and Indirect Environmental Effects. *Int J Environ Res Public Health* **19**, (2022).

53. Hirshfeld, S., Vesilindt, P. A. & Past, E. I. *ASSESSING THE TRUE COST OF LANDFILLS*. *Waste Management & Research* vol. 10 (1992).

54. Joshi, R. & Ahmed, S. Status and challenges of municipal solid waste management in India: A review. *Cogent Environmental Science* vol. 2 Preprint at https://doi.org/10.1080/23311843.2016.1139434 (2016).

55. Makarichi, L., Jutidamrongphan, W. & Techato, K. anan. The evolution of waste-to-energy incineration: A review. *Renewable and Sustainable Energy Reviews* vol. 91 812–821 Preprint at https://doi.org/10.1016/j.rser.2018.04.088 (2018).

56. Taghipour, H., Mohammadyarei, T., Jafarabadi, M. A. & Hashemi, A. A. On-site or off-site treatment of medical waste: A challenge. *J Environ Health Sci Eng* **12**, (2014).

57. EPA Medical Waste Incineration.

58. Zhao, L., Zhang, F. S., Chen, M., Liu, Z. & Wu, D. B. J. Typical pollutants in bottom ashes from a typical medical waste incinerator. *J Hazard Mater* **173**, 181–185 (2010).

59. Dharmaraj, S. *et al.* Pyrolysis: An effective technique for degradation of COVID-19 medical wastes. *Chemosphere* vol. 275 Preprint at https://doi.org/10.1016/j.chemosphere.2021.130092 (2021).

60. Sharifzadeh, M. *et al.* The multi-scale challenges of biomass fast pyrolysis and bio-oil upgrading: Review of the state of art and future research directions. *Progress in Energy and Combustion Science* vol. 71 1–80 Preprint at https://doi.org/10.1016/j.pecs.2018.10.006 (2019).

61. Su, G. *et al.* Valorisation of medical waste through pyrolysis for a cleaner environment: Progress and challenges. *Environmental Pollution* **279**, (2021).

62. Qureshi, M. S. *et al.* Pyrolysis of plastic waste: Opportunities and challenges. *J Anal Appl Pyrolysis* **152**, (2020).

63. Trautmann, N. & Olynciw, E. Compost Microorganisms. *https://compost.css.cornell.edu/microorg.html*.

64. Epstein, E. *INDUSTRIAL COMPOSTING Environmental Engineering and Facilities Management*. (2011).

65. Reducing the Impact of Wasted Food by Feeding the Soil and Composting. https://19january2017snapshot.epa.gov/sustainable-management-food/reducing-impact-wasted-food-feeding-soil-and-composting_.html#:~:text=Mature%20compost%20is%20a%20stable,piles%2C%20rows%2C%20or%20vessels.

66. Gray, K. R. & Biddlestone, A. J. *The Composting of Agricultural Wastes*. (1981).

67. Schaller, H. Sterol and steroid biosynthesis and metabolism in plants and microorganisms. *Comprehensive Natural Products II: Chemistry and Biology* **1**, 755–787 (2010).

68. Aagaard, K., Luna, R. A. & Versalovic, J. The Human Microbiome of Local Body Sites and Their Unique Biology. *Mandell, Douglas, and Bennett's Principles and Practice of Infectious Diseases* **1**, 11–18 (2014).

69. Rebollido, R. *et al.* MICROBIAL POPULATIONS DURING COMPOSTING PROCESS OF ORGANIC FRACTION OF MUNICIPAL SOLID WASTE. *Appl Ecol Environ Res* (2008).

70. Füleky, G. & Benedek, S. Composting to Recycle Biowaste. in 319–346 (2010). doi:10.1007/978-90-481-3333-8_12.

71. Muniyasamy, S., Anstey, A., Reddy, M. M., Misra, M. & Mohanty, A. Biodegradability and compostability of lignocellulosic based composite materials. *J Renew Mater* **1**, 253–272 (2013).

72. Wu, J. *et al.* Identifying the key factors that affect the formation of humic substance during different materials composting. *Bioresour Technol* **244**, 1193–1196 (2017).

73. Mehta, C. M., Palni, U., Franke-Whittle, I. H. & Sharma, A. K. Compost: Its role, mechanism and impact on reducing soil-borne plant diseases. *Waste Management* **34**, 607–622 (2014).

74. Nordahl, S. L., Preble, C. V., Kirchstetter, T. W. & Scown, C. D. Greenhouse Gas and Air Pollutant Emissions from Composting. *Environmental Science and Technology* vol. 57 2235–2247 Preprint at https://doi.org/10.1021/acs.est.2c05846 (2023).

75. Casella Organics, 'Hawk Ridge' Compost Facility. *https://composting.org/casella-organics-hawk-ridge-compost-facility/.*

76. Vozzola, E., Overcash, M. & Griffing, E. An Environmental Analysis of Reusable and Disposable Surgical Gowns. *AORN J* **111**, 315–325 (2020).

77. Reusable Isolation Gown. *Practicon* https://www.practicon.com/reusable-isolation-gown-white/p/7153611.

78. Uline Fluid-Resistant Gown. *ULINE* https://www.uline.com/Product/Detail/S-17099/Disposable-Clothing/Uline-Economy-Polycoated-Protective-Gown?pricode=WO622&AdKeyword=disposable%20ppe%20gowns&AdMatchtype=p&gad_source=1&gclid=CjwKCAiAi6uvBhADEiwAWiyRdpNx-L0oSFPRIl5Fyy3lTW5gHa2JYAqyIyUviZQk0Boy8bU8Cn6xohoCNqUQAvD_BwE.

79. MOXE Level 2 Disposable PPE Isolation Gowns. *Amazon* https://www.amazon.com/MOXE-Level-Disposable-Isolation-Gowns/dp/B08KTNYKCQ.

80. Isolation Gown AAMI Level 3. *USA Medical* https://www.usamedicalsurgical.com/isolation-gown-aami-level-3/.

81. Medline AAMI Level 3 Fluid-Resistant Heavyweight Isolation Gown. *Medline* https://athome.medline.com/en/medline-aami-level-3-fluid-resistant-heavyweight-isolation-gowns-shop-all-pf02344?utm_source=medline-pdp&utm_medium=referral&utm_campaign=SHOPNOW&utm_content=NONLV325H#228=1369&463=10337.

82. Reusable Level 2 Isolation Gowns. *Direct Textile Store* https://directtextilestore.com/Reusable-Level-2-Isolation-Gowns.

83. GoGreen Biodegradable Thumb Loop Isolation Gown. *Welmed* https://welmed.us/covid-19-ppe/gogreen-biodegradable-thumb-loop-isolation-gown-large-open-back-thumb-loop-wrists-made-in-the-usa/.

84. Biodegradable Disposable Isolation Gown. *Kingfa* https://www.medicalkingfa.com/products-detail/i-134.html.

85. Jian, J., Xiangbin, Z. & Xianbo, H. An overview on synthesis, properties and applications of poly(butylene-adipate-co-terephthalate)–PBAT. *Advanced Industrial and Engineering Polymer Research* vol. 3 19–26 Preprint at https://doi.org/10.1016/j.aiepr.2020.01.001 (2020).

86. Biogown. Biogown. https://thebiogown.com/.

87. Harbour Technologies. Harbour Technologies PPE Manufacturing. *https://www.harbour-tech.com/ppe-manufacturing/* (2023).

88. Mantrose-Haeuser Co., I. Food Packaging Coatings. *https://mantrose.com/products/food-packaging-coatings/*.

89. AATCC 42 Water Resistance: Impact Penetration Test. *AATCC* (2017).

90. AATCC 127 Water Resistance: Hydrostatic Pressure Test. *AATCC* (2017).

91. D5034 Standard Test Method for Breaking Strength and Elongation of Textile Fabrics (Grab Test). *ASTM* (2021) doi:10.1520/D5034-21.

92. D5733 Standard Test Method for Tearing Strength of Nonwoven Fabrics by the Trapezoid Procedure. *ASTM* (1999).

93. D1683 Standard Test Method for Failure in Sewn Seams of Woven Fabrics. *ASTM* (2022) doi:10.1520/D1683_D1683M-22.

94. D6868 Standard Specification for Labeling of End Items that Incorporate Plastics and Polymers as Coatings or Additives with Paper and Other Substrates Designed to be Aerobically Composted in Municipal or Industrial Facilities. *ASTM* (2021) doi:10.1520/D6868-21.

95. ISO 16929 Plastics - Determination of the degree of disintegration of plastic materials under defined composting conditions in a pilot-scale test. *ISO* (2021).

APPENDICES

Appendix A.1. List of microorganisms typically found in compost. Reproduced from Ref [64].

Microorganisms Identified in Composting

Bacteria

Aerobacter (aerogenes)
Bacillus megatherium
B. stearothermophilus
B. cereus
B. Mycoides

Pseudomonad sp.
(Seven isolates)
Flavobacterium sp.
Micrococcus sp.
Sarcina sp.
Cellumonas folia
Chondrococcus exiguus
Mycococcus virescens
M. fulvus
Thibacillus thiooxidans
T. denitrificans
Proteus sp.

Actinomycetes

Nocardia brasiliensis
Thermomonospora viridis
T. curvata
Micromonospora parva
M. vulgaris
Thermoactinomyces vulgaris
Actinoplanes sp.
Thermopolyspor polyspora
Pseudonocardia
Streptomyces violaceoruber
S. thermoviolaceus
S. rectus
S. thermofuscus
S. thermovulgaris
Thermomonospora fusca
T. glaucus

Fungi

Rhizopus nigricans
Rhizoctonia sp.
Geotrichum candidum
Mucor pusillus
Penicillum digitatum
Mucor racemosus
Torulopsis sp.
Aspergillus flavus
Absidia (ramosa)
Saccharomyces sp.
Pullularia sp.
Pythium sp.
Hanisenula sp.
Trichoderma koningi
Talaromyces (Penicillium) duponti
Stysanus stemonitis
Glibotrys (alaboviridis)
Humicola insolens
Humicola griseus var. *thermoideus*

Absidis orchidis
Rhizopus arrhizus
Candida (parapsilosis)
Cladosporium herbarum
Rhodotorula rubra
Aspergillus tamarii
Zygorhynchus vuilleminii
Trichosporon cutaneum
Verticillium sp.
Synecephalastrum sp.
Pichia sp.
Cylindrocaron sp.
Chaetomium (thermophile)
Lipomyces sp.
Sporotrichium thermophile
Fusarium moniliforme

Appendix A.2. Machine Schematic of Impact Penetration Head.

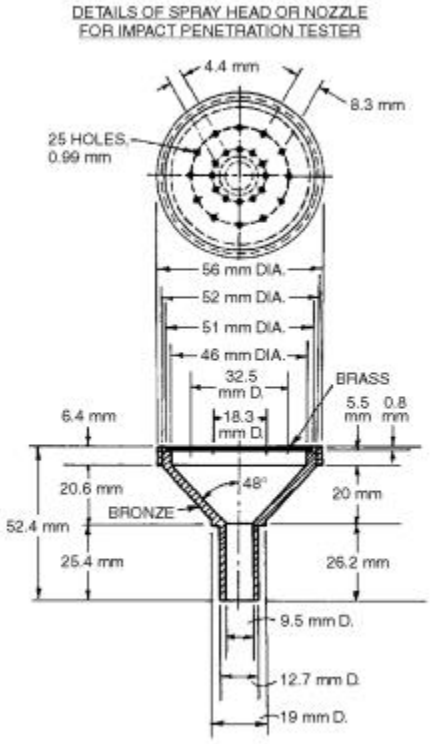

Fig. 4—Details of spray head.

BIOGRAPHY OF THE AUTHOR

Caden Scott, EI was born in Portland, Maine on August 14th, 2000. He was raised in Portland, Maine, and graduated from Deering High School in May 2018. In September 2018, Caden entered the University of Maine, majoring in Biomedical Engineering. Throughout his undergraduate career, he was heavily involved in research working in labs across the departments of Chemistry, Biology, and Biomedical Engineering. In his senior year, he passed the NCEES Fundamentals of Engineering exam and became an EI. Caden graduated *summa cum laude* with a B.S. in May of 2022 and shortly after joined the Neivandt Lab to develop a compostable isolation gown. Caden is a candidate for the Master's degree in Biomedical Engineering from the University of Maine in May 2024.